Title

lncRNA Epigenetic Landscape Analysis Identifies EPIC1 as an Oncogenic lncRNA that Interacts with MYC and Promotes Cell-Cycle Progression in Cancer

Journal

Cancer Cell, 33(4)

ISSN

1535-6108

Authors

Wang, Zehua
Yang, Bo
Zhang, Min
et al.

Publication Date

2018-04-01

DOI

10.1016/j.ccell.2018.03.006

Peer reviewed

HHS Public Access

Author manuscript

Cancer Cell. Author manuscript; available in PMC 2019 April 09.

Published in final edited form as:

Cancer Cell. 2018 April 09; 33(4): 706–720.e9. doi:10.1016/j.ccell.2018.03.006.

LncRNA epigenetic landscape analysis identifies *EPIC1* as an oncogenic lncRNA that interacts with MYC and promotes cell cycle progression in cancer

Zehua Wang[1,4], **Bo Yang**[1,4], **Min Zhang**[1], **Weiwei Guo**[1], **Zhiyuan Wu**[1], **Yue Wang**[1], **Lin Jia**[1], **Song Li**[1], **The Cancer Genome Atlas Research Network**, **Wen Xie**[1], and **Da Yang**[1,2,3,*,5]

[1]Center for Pharmacogenetics, Department of Pharmaceutical Sciences, University of Pittsburgh, Pittsburgh, PA 15261, USA

[2]University of Pittsburgh Cancer Institute, University of Pittsburgh, Pittsburgh, PA 15261, USA

[3]Department of Computational and Systems Biology, University of Pittsburgh, Pittsburgh, PA 15261, USA

Summary

We characterized the epigenetic landscape of genes encoding long noncoding RNAs (lncRNAs) across 6,475 tumors and 455 cancer cell lines. In stark contrast to the CpG island hypermethylation phenotype in cancer, we observed a recurrent hypomethylation of 1,006 lncRNA genes in cancer, including *EPIC1* (EPigenetically Induced lnCRNA1). Overexpression of *EPIC1* is associated with poor prognosis in luminal B breast cancer patients and enhances tumor growth *in vitro* and *in vivo*. Mechanistically, *EPIC1* promotes cell cycle progression by interacting with MYC through *EPIC1*'s 129–283 nt region. *EPIC1* knockdown reduces the occupancy of MYC to its target genes (e.g., *CDKN1A, CCNA2, CDC20*, and *CDC45*). MYC depletion abolishes *EPIC1*'s regulation of MYC target and luminal breast cancer tumorigenesis *in vitro* and *in vivo*.

Graphical abstract

*Correspondence: dyang@pitt.edu.
[4]These authors contributed equally
[5]Lead Contact

AUTHOR CONTRIBUTIONS

Conceptualization, D.Y., B.Y., Z.W.; Methodology, Z.W., B.Y., Z.M., and D.Y.; Formal Analysis, B.Y., Z.W., M.Z., W.G., Z.Y.W. and D.Y.; Investigation, Z.W., B.Y., M.Z., W.G., Z.Y.W., Y.W., L.J., W.X., S.L. and D.Y.; Resources, B.Y. and M.Z.; Writing – Original Draft, Z.W., B.Y., M.Z., W.X., and D.Y.; Writing – Review & Editing, Z.W., B.Y., M.Z., W.G., Z.Y.W., W.X., S.L. and D.Y.; Supervision & Funding Acquisition, D.Y.

DECLARATION OF INTERESTS

D.Y. and Z.W. are named inventors on a pending patent application describing the use of antisense oligonucleotides against specific *EPIC1* sequence as diagnostic and therapeutic tools.

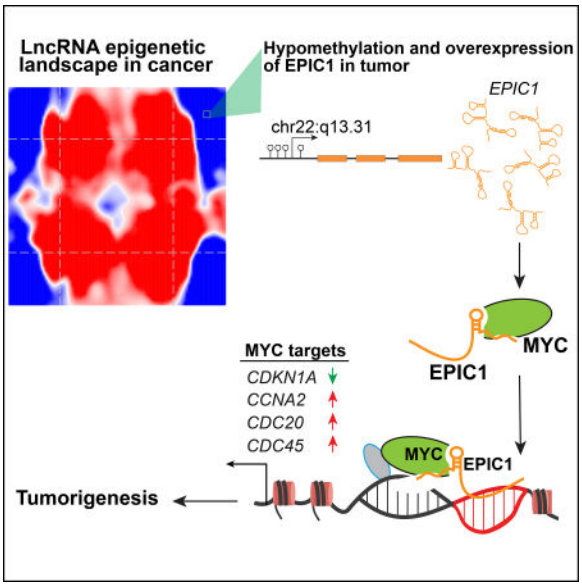

Introduction

The most recent genome-wide characterization of the human cancer transcriptome has demonstrated that lncRNA expression is among the most pervasive transcriptional changes in cancer (Du et al., 2013; Iyer et al., 2015). Further experimental evidence indicates that lncRNAs can play an important role in tumorigenesis (Du et al., 2016; Prensner and Chinnaiyan, 2011; Schmitt and Chang, 2016; Zhu et al., 2016). Similar to protein-coding genes (PCGs), lncRNA expression is subject to changes in gene dosage (e.g., copy number alterations) and promoter utilization (e.g., DNA methylation) that occur in cancer initiation and progression. In this regard, lncRNA genes can be targeted by cancer somatic alterations and thus play important roles in tumorigenesis. Recent studies focusing on the identification of copy number alterations (Hu et al., 2014; Leucci et al., 2016; Yan et al., 2015) and cancer risk polymorphism in promoter regions (Guo et al., 2016) of lncRNA genes have provided evidence demonstrating that somatic/germline alterations of lncRNA in tumors can be “driver molecular events” leading to tumor initiation and progression.

Epigenetic regulation is one of the major mechanisms utilized to control lncRNA expression and tissue specificity (Amin et al., 2015; Guttman et al., 2009; Wu et al., 2010). Epigenetic alterations have been established as one of the hallmarks of tumorigenesis (Jones and Baylin, 2002; Shen and Laird, 2013). However, the epigenetic alterations of lncRNA genes and their consequences in cancer remain poorly characterized. Genome-scale studies have yielded important insights into DNA methylation changes in tumors (Irizarry et al., 2009; Noushmehr et al., 2010) but have mostly focused on PCG promoters. The efforts to characterize the lncRNA epigenetic landscape in cancers have labored under the limitations of an imperfect annotation of lncRNAs and a dearth of platforms that can detect lncRNA epigenetic and expression alterations in cancer. The emergence of large-scale cancer genomic/epigenetic projects, such as The Cancer Genome Atlas (TCGA) Research Network

project, have provided an excellent opportunity to characterize the lncRNA epigenetic landscape in cancer.

Here, we repurposed and integrated multi-dimensional genomic and epigenetic data from TCGA, Cancer Cell Line Encyclopedia (CCLE) (Barretina et al., 2012), and Catalogue of Somatic Mutations in Cancer (COSMIC) (Iorio et al., 2016) projects to characterize the DNA methylation landscape of lncRNA genes across 33 cancer types. We aimed to build a detailed knowledge base and data analysis pipeline to explore DNA methylation alterations in lncRNA promoter in cancer. We hypothesize that if some lncRNA genes are recurrently targeted by DNA methylation alterations in tumors, they may play an important role in tumor initiation and progression. By further integrating with the TCGA clinical data and somatic alterations of well-documented cancer genes, we targeted to identify and mechanistically validate lncRNAs that may have a tumorpromoting or tumor-suppressing function.

Results

LncRNA promoters exhibit a distinct pattern of epigenetic alterations in cancer compared with protein-coding genes

To interrogate lncRNA DNA methylation in cancer, we developed a computational pipeline to repurpose HM450 probes to lncRNA promoters (Figures S1A and S1B). This analysis resulted in a set of 225,868 probes annotated to 28,366 genes. Specifically, 66,832 HM450 probes were annotated to 9,606 lncRNA genes (29,117 CpG islands), comprising approximately 60.4% of all lncRNAs in ENCODE annotation (Table S1). The lncRNAs that had at least one HM450 probe covering their promoters included 3,964 intergenic and 4,053 antisense lncRNA genes (Table S1). The median distances between lncRNA promoters and their nearest HM450 probes is 1,267 bp. The identified DNA methylation probes are mainly located within 3 kb regions of H3K4me3 and H3K27ac peaks of their mapped genes (Figure 1A) (Consortium, 2012), suggesting that the probes indeed represent the promoter methylation status of lncRNAs and PCGs (Shlyueva et al., 2014).

We first sought to determine the lncRNA DNA methylation pattern in cancer by comparing the DNA methylation profile of lncRNA promoters between tumors and normal tissues using the TCGA Pan-Cancer database (syn4382671, Table S1). Because the CpG island hypermethylation phenotype (CIMP) has been established as one of the hallmarks in many cancer types (Baylin et al., 1986), we originally expected to identify hypermethylated tumor-suppressing lncRNAs. Intriguingly, we observed both hypermethylated and hypomethylated lncRNA promoters in breast cancer tissues (Figures 1A and S1C). This observation is in stark contrast to the PCG promoters, which were predominantly hypermethylated in breast cancer (Figure 1A). Of the intergenic lncRNAs that do not share promoters with PCGs, there were 504 intergenic lncRNA promoters showing significant hypomethylation and 639 intergenic lncRNA promoters showing significant hypermethylation in breast cancer (false discovery rate [FDR] < 0.05 and effect size > 0.2). The hypomethylation pattern of lncRNA promoters was consistently observed in another nine cancer types that also had matched normal tissues available (Figures 1B and S1D). To determine if this observation was an artifact due to bias of the HM450 microarray design, we randomly permuted the labels of

lncRNAs and PCGs for 10,000 times and generated an empirical distribution to estimate the FDR for each promoter. This analysis revealed that the lncRNA promoters were significantly hypomethylated in all ten cancer types ($p < 10^{-15}$, K-S test, Figure 1C).

Integrative analysis identified 2,123 recurrent epigenetically regulated lncRNAs in 20 cancer types

To determine whether lncRNAs' expression is regulated by the DNA methylation changes at their promoters (e.g., hypomethylation causes overexpression), we integrated the lncRNA expression data from MiTranscriptome, which summarized the expression of 12,382 cancer-associated lncRNA transcripts using an *ab initio* assembly method in 6,475 RNA-seq profiles, including 5,602 TCGA samples (Iyer et al., 2015). Our analysis focused on TCGA samples across 20 cancer types that have both DNA methylation and lncRNA expression data. We applied a heuristic strategy to identify the lncRNAs that are epigenetically activated (EA) or silenced (ES) in tumors in comparison to their DNA methylation status in normal tissues. This method prioritized the lncRNAs that not only exhibited a significant difference in DNA methylation between tumors and normal tissues, but also exhibited expression changes highly correlated with their DNA methylation alterations (see details in STAR Methods). A patient-centric matrix with DNA methylation status of 2,123 lncRNA genes across 20 cancer types was characterized, including 1,006 EA and 1,117 ES lncRNAs that showed epigenetic alteration in at least one cancer type (Table S2). The top 20 most frequently EA and ES lncRNAs are shown in Figure 2A. All the epigenetically regulated lncRNAs, with either hypomethylation or hypermethylation in tumors, exhibited a significant negative correlation (FDR < 0.01) between their expression and promoter DNA methylation status (Figures 2B and 2C). Notably, a group of the EA lncRNAs in tumors was not expressed in normal tissues (Figure S2A). This "on or off" expression pattern of EA lncRNAs potentiated them as promising diagnostic biomarkers. To further validate the methylation status of the lncRNAs and their expression in cancer, we investigated the RNA-seq and HM450 DNA methylation profiles of 455 cancer cell lines from the CCLE and COSMIC databases (Barretina et al., 2012). Among the top 40 lncRNAs, 34 (14 EA and 20 ES lncRNAs) exhibited a similar expression pattern in cancer cell lines and significantly negative correlation between their expression and promoter methylation (Figures 2D and S2B, Table S2).

Epigenetically regulated lncRNAs are associated with tumor survival and proteincoding cancer gene alterations

We next analyzed the association of lncRNA epigenetic status with patient survival in 20 cancer types. Twelve of the top 20 EA lncRNAs were significantly correlated with poor survival in at least one cancer type, while ten of the top 20 ES lncRNAs were significantly correlated with favorable survival (Figures S2C–S2E). Among these survival-related lncRNAs are *SNHG12* and *MINCR*, which are epigenetically activated in multiple cancer types, including breast, bladder, endometrial, colorectal, and lung cancer (Figure 2A, Table S2). These lncRNAs have been documented to be overexpressed in a variety of cancer types and to play oncogenic roles in regulating cell proliferation and migration (Doose et al., 2015; Li et al., 2013; Ruan et al., 2016). To explore the relationship between lncRNA epigenetic alterations and the somatic alterations of known tumor genes, we integrated the

lncRNA epigenetic alterations with the mutation and copy number alterations of known protein-coding cancer genes in the same tumors (Vogelstein et al., 2013). Notably, the epigenetically regulated lncRNAs show a strong co-occurrence with a group of cancer gene mutations and copy number alterations (Figure S2F, Table S2). For example, EA lncRNAs are significantly enriched in *TP53* mutated tumors in multiple cancer types (Figures S2F and S2G). By contrast, ES lncRNAs exhibit significant mutual exclusivity with *EGFR* amplifications and mutations (Figure S2F).

EPIC1 is epigenetically activated and correlated with poor survival in breast cancer

The lncRNA that is most frequently epigenetically activated in multiple cancer types is ENSG00000224271 (EPigenetically Induced lnCRNA1, [*EPIC1*]) (Figure 2A). It is an intergenic lncRNA (CPAT coding probability = 0.004) located on chr22:q13.31. There are CpG islands within 164 bp downstream of this gene's transcription start site (TSS) (Figure 3A). This lncRNA is epigenetically activated in up to 90% of tumor samples across ten cancer types, including breast cancer (Figures 2A and 2D, Table S2). Our algorithm identified three probes in HM450 mapping to the *EPIC1* CpG islands (Figure 3A). Based on the beta values of three probes, three subgroups of breast cancer were identified by the hierarchical clustering analysis in 534 breast tumors (Figure 3B). The hypermethylated subgroup includes 196 (36.7%) breast tumors and exhibits a high *EPIC1* methylation level similar to that in normal breast tissues (Figure 3B). Breast tumors of this subgroup are characterized by reduced *EPIC1* expression (Figures 3C and 3D) and an improved overall survival in comparison to the other two groups (Figure 3E). In contrast, patients whose tumors exhibit *EPIC1* hypomethylation and increased *EPIC1* expression have the worst survival (Figures 3C–3E). To determine if *EPIC1* expression is robustly associated with poor patient survival in breast cancer, we re-annotated the probes from five Affymetrix microarrays to lncRNAs and identified one probe (1563009_at) in an Affymetrix HG-U133plus2 microarray that specifically detected *EPIC1* expression. As shown in Figure 3F, increased expression of *EPIC1* was consistently associated with poor survival in six independent patient cohorts, including 965 breast tumors (Figures 3F and S3A).

Further analysis revealed that *EPIC1* epigenetic activation is significantly associated with luminal B and HER2 subtypes of breast cancer ($p < 0.001$, Figures S3B and S3C). In 119 TCGA luminal B tumors, patients with *EPIC1* epigenetic activation demonstrated significant poor survival ($p = 0.002$, Figure S3D). The association between *EPIC1* and breast cancer poor survival remains significant after adjusting cancer subtypes along with other prognostic factors including age and clinical stage (multivariate Cox regression model $p = 0.02$). In all 20 cancer types assessed, *EPIC1* epigenetic activation is also significantly correlated with poor survival in endometrial cancer patients (UCEC, Figure S2C).

Using RNA-seq and HM450 DNA methylation data in the CCLE database, we observed a significant negative correlation ($p < 0.05$) between endogenous *EPIC1* expression levels and its promoter methylation in 24 breast cancer cell lines (Figures S3E and S3F). Among them, eighteen cell lines showed epigenetic activation of *EPIC1*, while four (i.e., MB231, HCC1937, CAMA1, and ZR-75-30) exhibited promoter hypermethylation and had low *EPIC1* expression (Figures S3E and S3F). Decitabine treatment caused a dosage- and time-

dependent *EPIC1* expression and demethylation in *EPIC1* hypermethylated cell lines (e.g., MB231), but not in cells that already exhibit *EPIC1* hypomethylation and overexpression (e.g., MCF-7) (Figures 3G, 3H, and S3G). Using a similar strategy, we selected seven other EA lncRNAs based on their novelty and demonstrated that decitabine treatment significantly induced EA lncRNAs expression by decreasing the DNA methylation level of their CpG islands (Figure S3H, Table S2).

To determine if *EPIC1* is directly regulated by DNA methylation, we cloned *EPIC1*'s promoter region (including the CpG islands) and performed *in vitro* DNA methylation assay (Figure 3I). Luciferase reporter assays revealed that the unmethylated *EPIC1* promoter (unMeth-*EPIC1*) led to a significantly higher reporter activity compared to the methylated version (Meth-*EPIC1*) ($p < 0.01$, Figure 3I). Collectively, these results demonstrated that *EPIC1* is directly regulated by DNA methylation at the CpG islands in its promoter region.

EPIC1 functions as a potential oncogenic lncRNA by promoting cell cycle progression

To evaluate the oncogenic role of *EPIC1* in cancer, we analyzed the *EPIC1* expression status in 28 cell lines across eight cancer types using qRT-PCR. In agreement with *EPIC1*'s activation in the luminal B breast cancer subtype, *EPIC1* is overexpressed in luminal breast cancer cell lines (e.g., BT-474, MB361, MCF-7, ZR-75-1, and T-47D) (Lehmann et al., 2011), along with ovarian cancer (A2780cis and OVCAR-4), pancreatic cancer (BxPC-3 and PANC-1), prostate cancer (PC-3), and leukemia (K562) cell lines (Figures S4A–S4C). We further performed 5'-RACE and 3'-RACE cloning using total RNA from MCF-7 and T-47D cells to identify functional *EPIC1* isoforms. Three splice variants of *EPIC1* were cloned, including isoform v1 (567 nt), isoform v2 (844 nt), and isoform v3 (882 nt) (Figures S4D–S4F). All of them share same exon 1 and exon 2. We designed six siRNAs targeting shared sequence of all isoforms and screened three siRNAs that can readily knock down *EPIC1* expression (Figure S4G). *EPIC1* knockdown resulted in a decrease of cell proliferation in a time-dependent manner in luminal breast cancer cells MCF-7 and ZR-75-1 (Figures 4A–4F). Soft agar assays further demonstrated that *EPIC1* knockdown significantly inhibits the anchorage-independent growth of cancer cells (Figure 4G). Moreover, cell cycle analysis revealed that silencing of *EPIC1* resulted in G_0/G_1 arrest in MCF-7 and ZR-75-1 cells (Figures 4C, 4F, and S4H). Next, we established stable *EPIC1* knockdown cells using lentiviral shRNAs. Both sh*EPIC1* stable cells exhibited significantly reduced cell proliferation (Figures S4I and S4J), anchorage-independent growth (Figure S4K), and *in vivo* xenograft growth (Figures 4H and 4I), compared to the shCtrl cells. These results not only suggest oncogenic activity of *EPIC1 in vivo,* but also provide a potential therapeutic target for breast cancer treatment.

EPIC1 is a nuclear lncRNA that regulates MYC targets

Cell fractionation PCR and subcellular RNA sequencing analyses revealed that *EPIC1* RNA is predominately located in the nucleus (Figures 5A, S5A, and S5B), suggesting that *EPIC1* might play a role in transcriptional regulation and chromatin interactions (Batista and Chang, 2013). To explore this possibility, RNA-seq analyses were performed on MCF-7 cells transfected with two siRNAs targeting *EPIC1* individually or pooled. We have confirmed that both siRNAs can readily knock down the level of nuclear *EPIC1* RNA

(Figure S5C). To exclude possible off-target effects on gene expression associated with single siRNAs, we focused only on genes regulated in the same direction in all three transfection experiments. *EPIC1* knockdown in MCF-7 cells resulted in the regulation of 805 genes (upregulation of 317 genes and downregulation of 488 genes) (Figure 5B, Table S3), which are highly overlapped with 2,005 *EPIC1*-associated genes that were significantly correlated with *EPIC1* expression across 559 TCGA breast tumors ($p = 2.6 \times 10^{-25}$, Figures 5B and 5C). This overlap was even higher in the pathway analysis. Gene Set Enrichment Analysis (GSEA) analysis showed that cell cycle related biological processes such as "MYC targets", "G2M checkpoint", and "E2F targets" were significantly enriched in the *EPIC1*-associated genes in 17 out of 20 cancer types (Figure 5D, Table S3). The same cellular processes were enriched in the *EPIC1*-regulated genes in MCF-7 cells (Figure 5D, Table S3). Among them, the MYC pathway / targets are prominent gene sets enriched with *EPIC1*-regulated genes in both tumor samples and cell lines (Figure 5E). For example, the MYC targets *CDC45, CDC20*, and *CCNA2* were significantly downregulated by *EPIC1* knockdown. Moreover, *CDKN1A* (encoding the p21 protein) was significantly induced after *EPIC1* knockdown (Figures 5F, 5G, and S5D). p21 is a well-established negative regulator of cell cycle progression at G_1 and S phase that is directly inhibited by MYC (Gartel and Radhakrishnan, 2005). These observations are consistent with our observation that *EPIC1* knockdown resulted in cancer cells' arrest at G_0/G_1 phase. Similarly, in MCF-7 and ZR-75-1 cells, MYC knockdown also led to a pattern of MYC target expression and cell growth comparable with *EPIC1* knockdown (Figures 5G and S5E–S5H). This suggested that the oncogenic role of *EPIC1* may be associated with MYC protein.

EPIC1 interacts with the 148–220 aa region of MYC through its 129–283 nt sequence

To study the interaction between *EPIC1* RNA and MYC protein, we overexpressed each of three *EPIC1* isoforms (i.e., v1, v2, and v3) with Flag-tagged MYC protein in 293T cells, and performed RNA immunoprecipitation (RIP) assay. This analysis revealed that *EPIC1* isoforms v1 and v2 could be enriched by MYC RIP (Figure S6A). In v1 or v2 isoforms overexpressing MCF-7 cells, only the v1 isoform could regulate MYC target genes (Figures S6B and S6C). We further observed that overexpression of the *EPIC1* v1 isoform promoted G_1 phase progression and *in vivo* xenograft growth (Figures S6D–S6F). It is apparent to us that the v1 isoform is the functional isoform of *EPIC1* gene in breast cancer. We therefore used isoform v1 (567 nt) as the reference sequence of *EPIC1* in the following study.

RNA pull-down assay showed that MYC protein could be co-precipitated by an *in vitro*-transcribed biotinylated *EPIC1* sense transcript, but not by the *EPIC1* antisense transcript (Figure 6A). MYC RIP with cell lysates from MCF-7 cells was then performed to confirm the interaction between endogenous *EPIC1* and MYC protein (Figures 6B, S6G, and S6H). A well-documented MYC interacting lncRNA, *PVT1* (Tseng et al., 2014), was included as positive control and could also be enriched by MYC RIP (Figure 6B). Further *in vitro* binding assay using *in vitro*-transcribed *EPIC1* RNA and recombinant His-tagged MYC protein demonstrated that *EPIC1* binds directly to MYC protein (Figure 6C). To map the *EPIC1* functional motifs corresponding to MYC binding, we conducted an *in vitro* RNA pull-down assay using a series of truncated *EPIC1* fragments. This analysis revealed that nucleotides 1–358 of *EPIC1* (*EPIC1* 1–358 nt) are sufficient to interact with MYC protein,

while other *EPIC1* truncated fragments could not (Figure 6D). To map with greater precision the sequence of *EPIC1* that binds to MYC, we further designed seven truncated or deletion mutants of the *EPIC1* 1–358 nt region and revealed that three deletion mutants (Δ121–180 nt, Δ181–240 nt, and Δ241–300 nt) can abolish *EPIC1* binding to MYC protein. Deletion of all three regions (129–283 nt) also abolished *EPIC1*'s interaction with MYC protein (named as *ΔMYC-EPIC1*, Figures 6E and 6F). These data suggested that the *EPIC1* 129–283 nt region is necessary for *EPIC1*'S binding to the MYC protein. MYC protein domain mapping studies revealed that *EPIC1* binds the 148–220 amino acid (aa) region of MYC, which is not overlapped with the well-characterized transcriptional activation domain (TAD) and basic helix-loop-helix (bHLH) domain of MYC protein (Luscher, 2001; von der Lehr et al., 2003) (Figures 6G and 6H). Deletion of the 148–220 aa region of MYC protein (named as ΔEPIC1-MYC) abolished its interaction with *EPIC1* (Figures 6G and 6H). Collectively, our findings demonstrated that *EPIC1* interacts with the 148–220 aa region of MYC through its 129–283 nt sequence.

The oncogenic role of *EPIC1* partially depends on its regulation of MYC occupancy on target promoters

With the observation that *EPIC1* directly interacts with MYC, we further analyzed the effect of *EPIC1* on MYC target gene reporters (e.g., *p21* and *CCNA2* promoters) in MCF-7 cells. The reporter assays revealed that knockdown of either *EPIC1* or *MYC* significantly regulates p21-Luc and CCNA2-Luc reporter luciferase activities (Figure 7A). These observations indicate that *EPIC1* directly regulates the expression of MYC targets through their promoter regions. Interestingly, *EPIC1* knockdown had little effect on the expression of MYC (Figure 5G), which led to our hypothesis that *EPIC1* may regulate the transcriptional activity of the MYC protein.

To test this hypothesis, we performed an integrated analysis on MYC chromatin immunoprecipitation (ChIP)-seq data (Lee et al., 2012) and RNA-seq data of *EPIC1* knockdown MCF-7 cells. Among 805 *EPIC1*-regulated genes, 785 have robust MYC occupancy on their promoters in two biological replicates of MCF-7 ChIP-seq data. Interestingly, we did not observe a significant correlation between global MYC binding affinity and differentially expression (i.e., fold change) after *EPIC1* knockdown in MCF-7 cells, suggesting that *EPIC1* may regulate MYC's occupancy on a specific group of targets. By further considering previously validated MYC targets (Li et al., 2003; Zeller et al., 2006), we identified 40 possible targets of the *EPIC1*-MYC regulatory axis (Figures 7B and S7A, Table S4). ChIP-qPCR were performed and validated that *EPIC1* knockdown significantly reduces MYC's occupancies on the promoters of 26 targets, including *CDKN1A (p21), CCNA2, CDC20, and CDC45* (Figures 7C, S7B, and S7C). It is known that MYC binds to DNA and functions as a transcription factor by heterodimerization with another transcription factor, MAX (Amati et al., 1993; Blackwood and Eisenman, 1991). MYC and MAX Co-IP assay in MCF-7 cells revealed that *EPIC1* knockdown could moderately reduce the formation of MYC-MAX complexes (Figure S7D). Moreover, overexpression of *EPIC1*, but not *ΔMYC-EPIC1*, could enhance the reporter luciferase activities mediated by MYC and MAX (Figure S7E). These results suggest that *EPIC1* promotes MYC's occupancy on *EPIC1*-regulated genes through its 129–283 nt sequence (i.e., MYC-binding sequence).

To further determine the role of the *EPIC1*-MYC regulatory axis in cancer, we performed the MYC knockdown in *EPIC1* stably overexpressing MCF-7 cells, and observed that *EPIC1* regulation of cell proliferation and MYC target expression were attenuated by MYC knockdown (Figures 7D and 7E). Overexpression of MYC, but not *EPIC1*-binding deficient mutant MYC proteins (ΔEPIC1-MYC), regulates CCNA2 and p21 expression (Figure S7F). We further depleted the endogenous *EPIC1* expression using locked nucleic acid (LNA) in MCF-7 cells, followed by overexpression of either LNA-resistant wild-type *EPIC1* (WT-*R-EPIC1*) or deletion mutant of 129–283 nt MYC binding region (*ΔMYC-R-EPIC1*). Similar to *EPIC1* siRNA treatment, LNA knockdown of *EPIC1* significantly caused G_1 arrest of MCF-7 cells, which could be rescued by reintroduction of full-length *EPIC1*, but not *ΔMYC-EPIC1* (Figures 7F and S7G). The expression of full-length and the truncated *EPIC1s* were confirmed to be comparable levels to rule out the influence of transfection efficiency (Figure 7G). Consistently, LNA knockdown of *EPIC1* also curtailed the expression of MYC target genes. Reintroduction of wild type *EPIC1*, but not *ΔMYC-EPIC1*, was able to rescue the regulation of these genes (Figure 7G). These results suggested that the oncogenic role of *EPIC1* is at least in part dependent on its interaction with the MYC protein.

Discussion

Previous studies, by repurposing copy number and gene expression microarray data, have successfully identified the copy number alterations (Hu et al., 2014; Leucci et al., 2016; Tseng et al., 2014; Yan et al., 2015) and expression alterations of lncRNA (Du et al., 2013) in cancer. In the present study, we repurposed and integrated multidimensional genomic and epigenetic data from 6,475 tumor samples and 455 cancer cell lines in the TCGA and CCLE projects. These data were remapped/realigned to 9,606 annotated human lncRNAs to comprehensively characterize the lncRNA epigenetic landscape in cancer. Our analyses demonstrate that integrating HM450 microarray and RNA-seq data is a cost-effective strategy to research the DNA methylation regulation of lncRNA genes given the large number of HM450 and RNA-seq datasets available in public repositories. Our study has revealed that lncRNAs can be epigenetically activated in tumors by loss of DNA methylation in the promoter region, which is in stark contrast to the well-documented CIMP phenotype of protein coding genes in tumors. By further integrating with the protein-coding cancer gene alterations in same tumors, we observed that lncRNA epigenetic activation exhibited a strong co-occurrence with *TP53* mutation in multiple cancer types. Emerging evidence has demonstrated that p53 is a master regulator of lncRNAs' expression in cancer (Sanchez et al., 2014; Schmitt et al., 2016). Future study is warranted to determine whether loss of DNA methylation makes the promoters of these lncRNAs accessible to transcription factors, such as p53, and leads to transcriptional activation.

We hypothesize that if some lncRNAs are recurrently targeted by epigenetic alterations in tumors, they may play an important role in tumor initiation and progression. Indeed, the epigenetically regulated lncRNAs identified in this study include a number of known cancer-related lncRNAs, such as *KCNQ1OT1* (Engel et al., 2000), *MEG3* (Zhou et al., 2012), *MINCR* (Li et al., 2013), *HOTAIR* (Gupta et al., 2010), and *WT1-AS* (Hancock et al., 2007). Consistent with their somatic DNA methylation alterations identified in this study,

germline epigenetic defects in some of those lncRNAs have been documented to cause predisposition to Wilms tumor (Scott et al., 2008) and pediatric adrenocortical tumors (Wijnen et al., 2012).

Encouraged by the recapitulation of documented cancer-related lncRNAs, we mechanistically validated the most frequently epigenetically activated gene, *EPIC1*, as a potential oncogene. We have demonstrated that *EPIC1* interacts with MYC protein through its 129–283 nt region and increases MYC occupancy on *EPIC1*-regulated genes. The oncogenic role of MYC has been well documented in cancer initiation and progression (Dang, 2012). As an oncogene, *MYC* can be activated by multiple mechanisms in cancer. Chromosomal rearrangement is believed to be the most common genetic alteration of *MYC* (Dang, 2012). Other MYC activation mechanisms include transcriptional regulation, mRNA stabilization, and protein overexpression and stabilization (Kress et al., 2015). Emerging evidence uncover lncRNA's role for MYC activation in cancers. Three recent reports identified lncRNA *CCAT1-L* (Colorectal Cancer Associated Transcript 1), *GHET1* (Gastric Carcinoma Highly Expressed Transcript 1), and *PCGM1* (Prostate Cancer Gene Expression Marker 1) to be involved in modulating the transcription (Xiang et al., 2014) or RNA stability (Yang et al., 2014) of MYC in colorectal, gastric and prostate cancers (Hung et al., 2014). Another study demonstrated lncRNA *PVT1* (Plasmacytoma Variant Translocation 1) as an oncogenic lncRNA that interacts and stabilizes the MYC protein (Tseng et al., 2014).

However, little is known about whether and how lncRNAs regulate the transcriptional activity of MYC. MYC protein alone cannot form a homodimer nor bind to DNA *in vivo*. In most cases, MYC heterodimerizes with a partner protein, MAX (Amati et al., 1993; Blackwood and Eisenman, 1991) via a basic-helix-loop-helix-leucine zipper (bHLH-LZ) domain. The MYC-MAX complex binds directly to DNA sequence (CACA/GTG), which is a subset of the general E-box (CACGTG) DNA recognition sequence and functions as transcriptional activator or repressor (Blackwood and Eisenman, 1991; Luscher, 2001). It has been reported that MYC is bound to ~25,000 sites in the human genome (Cawley et al., 2004; Fernandez et al., 2003). Among those *in vivo* MYC binding sites, only a small set of sites have a MYC-MAX consensus CACA/GTG sequence (Fernandez et al., 2003). One reason for this discrepancy is that MYC can be recruited to non-canonical binding sites by other transcription factors. For example, MYC can interact with Miz1, which recruits MYC to its core promoter sequences that lack a MYC-MAX binding motif (Peukert et al., 1997). Other proteins, which recruit MYC to their cognate DNA binding sites, include specificity protein-1 (Sp1) (Gartel et al., 2001), nuclear factor Y (NF-Y) (Izumi et al., 2001), transcription factor II-I (TFII-I) (Roy et al., 1993) and yingyang-1 (YY1) (Shrivastava et al., 1993) . In the current study, our results suggest that *EPIC1* specifically regulates MYC's occupancy on a subset of MYC targets. Our results also showed that *EPIC1* can moderately enhance MYC-MAX interaction. It is possible that *EPIC1* only influences MYC's occupancy on canonical MYC-MAX binding sites, but not the non-canonical MYC binding sites mediated by other 'tethering factors'. Another possible explanation is that *EPIC1* may function as a "guide" RNA to facilitate MYCMAX's regulation on specific targets by directly binding to double-strand DNA. Future study is required to further define how *EPIC1* regulates MYC's occupancy on these specific MYC targets.

In summary, the establishment of a detailed knowledge base of the DNA methylation-altered lncRNAs in cancer will facilitate the identification of cancer-driving lncRNAs. Moreover, the mechanistic characterization of *EPIC1* and its functional crosstalk with the well-established oncogene *MYC* may help to pave the way to develop cancer therapies that target MYC through its interaction with *EPIC1*. The strong prognostic association of *EPIC1*, the robust tumor growth suppression by the *EPIC1* knockdown, and the illustration of *EPIC1*'s mechanism to promote breast cancer will shed light on the future development of lncRNA-based breast cancer therapies.

STAR*METHODS

CONTACT FOR REAGENT AND RESOURCE SHARING

Further information and requests for resources and reagents should be directed to and will be fulfilled by the Lead Contact, Da Yang (dyang@pitt.edu).

EXPERIMENTAL MODEL AND SUBJECT DETAILS

Data collection—DNA methylation, PCG expression, whole-exome mutation and GISTIC copy number alteration data were downloaded from TCGA Pan-Cancer project (Data Freeze 1.3). The lncRNA annotation was downloaded from GENCODE (V22, GRCh38). There were 7,656 intergenic, 5,565 antisense, and 920 sense intronic lncRNAs. H3K4me3 and H3K27ac ChIP-seq data for seven cell lines were downloaded from the UCSC genome browser: Integrated Regulation from ENCODE Tracks. DNA methylation data for breast cancer cell lines were downloaded from GSE57342 (Li et al., 2014) and GSE44837 (Di Cello et al., 2013).

RNA-seq data from 781 cancer cell lines in the CCLE database were downloaded from Expression Atlas (E-MTAB-2770). HM450 DNA methylation profile of 1,028 cancer cells lines form COSMIC database (Iorio et al., 2016). There are 455 cells which have both HM450 DNA methylation and RNA-seq data. The BAM files of RNA-seq of 939 breast cancer tumors were downloaded from Cancer Genomics Hub.

Mapping the probes to GENCODE genes—The genomic coordinates of HM450 probes based on GRCh37 were first transferred to genomic coordinates in GRCh38 using LiftOver (UCSC genome browser). We then searched the nearest TSS of PCG and lncRNA for each probe based on GENCODE V22 annotation. In this way, we defined: (1) the PCG probes, located in the PCG promoter region (+/− 3 kb from the TSS); (2) the lncRNA probes, located in the lncRNA promoter region; (3) the shared probes, located in both the PCG and lncRNA promoter regions; and (4) the non-probes, which are not located in any promoter regions (Figure S1B).

DNA methylation dysregulation pattern analysis in cancers—DNA methylation dysregulation in cancers showed a different beta value pattern in lncRNA promoter and protein-coding promoter regions. To evaluate the statistical significance of the difference between methylation in lncRNA and PCG promoter regions, we permuted the annotation for each probe 10,000 times to generate an experimental distribution of DNA methylation

change. Through comparison with the experimental distribution, an empirical p value could be calculated. Finally, the weighted twodimensional kernel density estimation R function *kde2d.weighted* (package: ggtern) was used to measure the distribution of hypomethylation or hypermethylation according to the distance to promoters of lncRNA and PCGs.

MiTranscriptome data renormalization—Recent reports have revealed that highly expressed genes affect the normalization scale much more and cause a bias against low-expression genes such as lncRNAs (Li et al., 2010; Wagner et al., 2012). To precisely evaluate the alteration of lncRNA expression in tumors, we renormalized the MiTranscriptome profile using a method similar to that described in S. Anders et al. (Anders and Huber, 2010). Specifically, a scaling factor for each sample was calculated as the median of the expression ratio to a pseudo-reference sample for each gene. The pseudo-reference sample was computed as the median expression level across all samples for that gene.

The formula to calculate the i-th sample's scaling factor:

$$scale_i = median_{j=1\ldots n}\left(\frac{E_{ij}}{median_{i=1\ldots m}(E_{ij})}\right)$$

where E indicates the expression profile, which has m samples and n genes. The denominator of the formula can be interpreted as j-th gene expression level of the pseudo-reference sample.

Characterization of the lncRNA landscape—We used a strategy similar as described in TCGA Glioblastoma project (Iorio et al., 2016) to characterize the epigenetic lncRNA landscape in each cancer type, which has successfully generated a patient-centric matrix for PCGs in glioblastoma using an Infinium HumanMethylation27 microarray. We adapted the strategy to accommodate for the lncRNA genes and the HumanMethylation450 microarray. Specifically, we first identified lncRNA and HM450 probe pairs in which the probe located at the lncRNA's promoter region as described previously. Then Spearman correlation coefficients (Rho) between the methylation alteration and gene expression for each lncRNA and probe pair were calculated for each cancer type. The probe with highest coefficient was selected for the lncRNA if multiple probes annotated to same gene promoter to capture the most variable and correlated probe for each gene. This procedure reduced the number of CpG probes from N:1 to 1:1. Next, we assigned discrete categories based on the Spearman correlation coefficient according to the following criteria:

1. Strongly negatively correlated (SNC) when the rho value was less than −0.5;
2. Weakly negatively correlated (WNC) when the rho value was between −0.5 and −0.25;
3. No negative correlation (NNC) when the rho value was greater than −0.25.

Next, we assigned samples to either the 30th (T30 or N30) or 70th (T70 or N70) percentile based on the observed beta value across tumor (T) and normal (N) samples. For a cancer type with less than 30 normal samples, we randomly selected 24 normal samples from each

of the three different normal tissues (72 samples in total). The three different normal tissues selected for this analysis were generated by TCGA for breast (BRCA), kidney (KIRC) and lung (LUSC) tumor studies. We finally scored each lncRNA gene per cancer type per tissue type (tumor and normal) according to the following rules:

1. If percentile 70 < 0.25, we score it as CUN or CUT (constitutively unmethylated in normal or tumor tissue);
2. If percentile 20 > 0.75, we score it as CMN or CMT (constitutively methylated in normal or tumor tissue);
3. If percentile 20 > 0.25 and percentile 70 < 0.75, we score it as IMN or IMT (intermediately methylated in normal or tumor tissue);
4. If it did not fall into any of the above categories, it was scored VMN or VMT (variably methylated in normal or tumor tissue).

Next, we assigned a ‘call' and a confidence ‘score' for each of the possible combinations (48) [3 (SNC, WNC, NNC) × 4 (CUN, CMN, VMN, IMN) × 4 (CUT, CMT, VMT, IMT)] per platform, as shown in Table S5. The methylation calls are as follows:

EA: Epigenetically activated

ES: Epigenetically silenced

UC: No Change

Methylation class confidence scores varied from EAH (epigenetic activation with high confidence), EAL (epigenetic activation with low confidence), NC (no change), ESL (epigenetic silencing with low confidence) and ESH (epigenetic silencing with high confidence) here. In this way, we generated a Methylation Patient-Centric Table of DNA methylation calls for each sample per lncRNA in 20 cancer types, and calculated the percentage of four types’ methylation status for each lncRNA in each cancer type.

The lncRNAs were ranked by summarized weighted alteration percentages among all the cancer types. Specifically, we give the EAH percentage with weight 2, EAL percentage with weight 1, UC percentage with weight 0, ESL percentage with weight −1, and ESH percentage with weight −2. The summarized weighted percentages of each lncRNA was used as a rank score. Generally, lncRNAs with consistent EA status in multiple cancer types would get a higher score, and the lncRNAs with consistent ES status in multiple cancer types would show a lower score.

Gene set enrichment analysis (GSEA)—To interpret the function of regulated genes after *EPIC1* siRNA treatment, GSEA (version 2.2.0) (Subramanian et al., 2005) was performed using the 50 cancer hallmark gene sets and a gene log2-fold change. To identify the pathways that are correlated with *EPIC1* expression in tumor samples, we performed a similar GSEA for each cancer type in TCGA dataset. In this analysis, GSEA was performed on the ranked PCG list based on the Spearmen's correlation coefficient with *EPIC1* expression.

RNA-seq data analysis—We developed a STAR-RSEM pipeline, which was revised from the ENCODE RNA-seq analysis pipeline. We used this pipeline to profile TCGA breast cancer and CCLE breast cancer cell line RNA-seq data, and the RNA-seq data of MCF-7 cells after *EPIC1* knockdown. To transfer the bam file to fastq, we used Picard-tools SamToFastq module. FastQC was used to check the sequencing quality. The RNA-seq data can be downloaded from GEO (GSE98538).

Association analysis between lncRNA epigenetic landscape and protein-coding gene alteration—Somatic mutations and copy number alterations in 32 cancer types were obtained from TCGA Pan-Cancer project (http://cancergenome.nih.gov/tcga/). The somatic mutations were identified via the MC3 algorithm. The copy number alterations were called using the GISTIC algorithm. An alteration profile of 32 cancer types was constructed. The columns of the alteration profile represent the samples, and the rows represent the tumor genes. If a gene was detected with alterations (non-synonymous somatic mutation or SCNA) in a sample, we set the profile to 1. Otherwise, the profile was set to 0.

For each PCG-lncRNA pair (denoted as G_i and L_i), we calculated the probability $P_{(Gi, Li)}$ of observing at least the number of samples that simultaneously contain alterations in both G_1 and L_i at random according to equation (1):

$$P_{(G_1, L_i)} = 1 - \sum_{k=0}^{a-1} \frac{\binom{a+b}{k}\binom{c+d}{a+c-k}}{\binom{n}{a+c}} \quad (1)$$

where n is the total number of samples, a is the number of samples with alterations in both genes, b is the number of samples with alterations only in G_1, c is the number of samples with alterations only in L_i, and d is the number of samples without alterations in either gene. The "hypergeometric test" p value was subjected to a Benjamini and Hochberg correction for multiple tests, and gene pairs with a FDR less than 0.05 were included in the following analysis.

Statistical and Clustering Analysis—Student's *t*-test, analysis of variance, chi-square, Wilcoxon rank-sum test, Fisher's exact test, Kaplan-Meier estimate, and Mantel-Cox survival analyses were performed using R 2.10.0. Significance was defined as $p < 0.05$. Benjamini-Hochberg multiple testing correction (Benjamini and Hochberg, 1995) was used to estimate the FDR when multiple testing correction was applied.

Integrating ChIP-seq and RNA-seq data to identify and validate *EPIC1*-MYC axis target gene—The genome-wide MYC protein binding sites were identified by applying Cistrome algorithm (Mei et al., 2017) on two biological replicates of MYC ChIP-seq assays of MCF-7 cells (Lee et al., 2012). We identified MYC targets that regulated by *EPIC1* based on two criteria: (1) at least one MYC binding peak falls within the TSS-proximal region (from 3 kb upstream to 500 bp downstream) of the gene; and (2) the gene is differentially expressed between the si*EPIC1* and control MCF-7 cells. The top targets of

EPIC1-MYC axis were selected based on their significance of MYC binding signal, differential expression after *EPIC1* knockdown, and their roles in cell proliferation/cycle. For each target, primers were designed to target the MYC binding region, and detailed primer sequences are listed in Table S5. ChIP-qPCR was further performed to demonstrate whether *EPIC1* knockdown decreases the recruitment of MYC to its target promoter sites.

Cell culture, RNA interference, LNA transfection, and plasmid transfection— Human breast epithelial cell line, MCF10A, and human breast cancer cell lines, BT-20, BT-474, HCC1937, Hs578T, MCF-7, MDA-MB-231 (MB231), MDA-MB-361 (MB361), MDA-MB-468 (MB468), T-47D, and ZR-75-1, and human ovarian cancer cell lines, SKOV-3, and NIH: OVCAR-3, and human pancreatic cancer cell lines, AsPC-1, BxPC-3, and PANC-1, and human prostate cancer cell lines, DU 145, and PC-3, and human leukemia cell line K562, and human lung cancer cell line A549, and human cervical cancer cell line HeLa, and human liver cancer cell line Hep G2, and human embryonic kidney (HEK) 293T cells were purchased from American Type Culture Collection (ATCC) and cultured as suggested by ATCC's guidelines. Human ovarian cancer cell lines, IGROV-1, OVCAR-4, and OVCAR-8 were purchased from NIH/NCI and kept in RPMI 1640 medium supplemented with 10% fetal bovine serum (FBS), 1% penicillin, and 1% streptomycin. The A2780 human ovarian cancer cell line and the cisplatin resistant version of the cell line, A2780cis, were obtained from the European Collection of Cell Cultures (ECACC), supplied by Sigma-Aldrich, and cultured in RPMI 1640 medium supplemented with 2 mM glutamine, 10% FBS, 1% penicillin, and 1% streptomycin; A2780cis cells were also supplemented with 1 μM cisplatin. Human pancreatic duct epithelial cell line (HPDE), and phoenix cells were kindly provided by Dr. Wen Xie (Department of Pharmaceutical Sciences, University of Pittsburgh), and HPDE cells were maintained in Keratinocyte-SFM medium supplemented with human recombinant epidermal growth factor and bovine pituitary extract (ThermoFisher, #17005042) and phoenix cells were maintained in DMEM supplemented with 10% FBS, 1% penicillin, and 1% streptomycin.

For RNA interference, cells were transfected with 40 nM siRNA targeting *EPIC1, MYC*, or a control siRNA using Lipofectamine RNAiMAX (ThermoFisher, #13778150) per the manufacturer's instructions. Total RNA was isolated 72 hr later for real-time PCR analysis. The siRNA sequences are listed in Table S5. For LNA transfection, cells were transfected with 40 nM LNA oligos targeting *EPIC1*, and a scramble control using Lipofectamine™ RNAiMAX per the guidelines. The LNA oligos were designed and synthesized from Exiqon, and detailed sequences are listed in Table S5.

For plasmid transfection, cells were transfected with plasmid using Lipofectamine™ 2000 (ThermoFisher, #11668019) or Lipofectamine™ 3000 (ThermoFisher, #L3000015) as suggested approaches.

Antibodies—The following antibodies were used for immunoblotting: rabbit anti-SNRP70 (Abcam, #ab83306), rabbit anti-GAPDH (Santa Cruz, #sc-25778), rabbit anti-MYC (Cell Signaling, #13987), rabbit anti-p21 (Cell Signaling, #2947), rabbit anti-CDC20 (Cell Signaling, #14866), rabbit anti-FLAG (Cell Signaling, #14793), rabbit anti-CDC45 (Cell Signaling, #11881), rabbit anti-MAX (Novus, #NBP1-49963), mouse anti-Cyclin A2 (Santa

Cruz, #sc-596), and mouse anti-β-actin (Sigma, #A5441). The following antibodies were used for co-immunoprecipitation (Co-IP), RNA immunoprecipitation (RIP) and chromatin immunoprecipitation (ChIP) analysis: rabbit anti-MYC (Santa Cruz, #sc-789), rabbit anti-MAX (Santa Cruz, #sc-764), rabbit anti-MYC (Cell Signaling, #9402), and normal rabbit IgG (Cell Signaling, #2729) as a negative control, and anti-FLAG M2 affinity gel (Sigma, #A2220).

Cell fractionation, cytoplasmic/nuclear RNA isolation—MCF-7, Hs578T, and T-47D cells were subjected to cytoplasmic and nuclear fractionation using a PARIS™ kit (ThermoFisher, #AM1921), and total RNA was isolated from each fraction following the recommended protocol.

RNA isolation and quantitative real-time PCR (qRT-PCR) assays—Total RNA was isolated from cultured cells using an RNeasy Mini kit (Qiagen, #74104) according to the manufacturer's instructions. cDNAs were synthesized from 0.5 μg of total RNA using a High-Capacity cDNA Reverse Transcription Kit (Applied Biosystems, #4368813). Real-time PCR was performed with *Power* SYBR Green PCR Master Mix (Applied Biosystems, #4367659) on a QuantStudio 6 Flex Real-Time PCR System (Applied Biosystems). Relative gene expression was determined by ΔΔCt normalized to *GAPDH*. The primers used are listed in Table S5.

***EPIC1* RNA copy number analysis—**Total RNA was isolated from 1×10^6 cells using an RNeasy Mini kit. The full-length of *EPIC1* RNA was *in vitro* transcribed with Ribonucleotide solution set (NEB, #N0450) and T7 RNA polymerase (Roche, #10881775001) using the PCR products as a template, treated with RNase-free DNase I (Promega, #M198A), and then isolated with the RNeasy Mini kit. cDNA was synthesized using 1μg of the total RNA or full-length of *EPIC1* RNA. Serial ten-fold dilutions (10^2 to 10^9 molecules per μl) of cDNA from *in vitro*-transcribed *EPIC1* RNA were used as a reference molecule for the standard curve calculation. Real-time PCR was performed as above.

Cloning, shRNA construction, and lentiviral transduction—Full-length of *EPIC1* was identified and amplified from total RNAs of MCF-7 / T-47D cells by 5'RACE and 3'-RACE using FirstChoice RLM-RACE Kit (ThermoFisher, #AM1700). To construct retroviral *EPIC1* expression plasmids, PCR products containing the CMV-zsGreen1 portion of pLncEXP (Addgene plasmid # 64865) were inserted into a pBABE puro vector (Addgene, #1764), and the resulting construct was named as pBABE-lnc. Then full-length and truncated mutants of *EPIC1* were cloned into pBABE-lnc with *Age*I and *Xho*I enzymes or cloned into pCDH-CMV-MCS-EF1-Puro (System Biosciences, #CD510B-1) with *Xba*I and *Eco*RI enzymes. Full-length of Flag-tagged or HA-tagged MYC expression vectors were generated using a human MYC cDNA Clone (OriGene, #SC112715) as a DNA template. Full-length of HA-tagged MAX expression vector was generated using cDNA from MCF-7 cells as a template. The truncated or deletion mutants and LNA-resistant *EPIC1* expression vectors were constructed by using QuickChange II XL Site-Direct Mutagenesis Kit (Agilent

Technologies, #200522). All constructs were confirmed by DNA sequencing at Genomics Research Core, University of Pittsburgh.

To construct stable *EPIC1*-expressing cells, pBABE-lnc and lnc-*EPIC1* plasmids were transfected into Phoenix cells to produce retrovirus, and viruses were collected 48 hr post-transfection. MCF-7 cells were infected for 24 hr with the retroviruses and selected with puromycin to establish stable *EPIC1*-expressing cells. Detailed sequences of primers used for cloning are listed in Table S5.

EPIC1 knockdown constructs were cloned by inserting oligos into a pLKO.1 TRC cloning vector (Addgene, #10878). The oligo sequences are listed in Table S5. To produce lentiviral particles, HEK 293T cells were seeded into one 6-cm Petri dish in DMEM with 10% FBS without antibiotics and incubated overnight to reach approximately 80% confluence before transfection. Transfection was performed using Lipofectamine 2000 Transfection Reagent according to the recommended protocol. Then, 3 μg of pLKO.1 shControl (shCtrl) or pLKO.1 sh*EPIC1* plasmid, 2.25 μg of psPAX2 (Addgene, #12260), and 0.75 μg of pVSV-G (Addgene, #8454) were used for each 6-cm petri dish. After transfection for 6 hr, the medium was changed with fresh DMEM containing 10% FBS, and the cells were incubated for another 48 hr. Culture medium containing the lentiviral particles was collected and filtered through a 0.45 μm filter to remove any remaining cells and debris. Target cells were infected for 24 hr with lentiviral particles in the presence of 8 μg/ml polybrene and screened with puromycin to establish stable cells.

Promoter cloning and reporter assay—Using genomic DNA from MCF-7 cells as DNA templates, the promoter region of *CCNA2* ranging from −443 bp to +334 bp was amplified by PCR and inserted to pGL3 Basic vector (Promega, #E1751) with *Nhe*I and *Hin*dIII enzymes, named as CCNA2-Luc, and the promoter region of *EPIC1* ranging from −133 bp to +587 bp were inserted to pGL3 Basic vector with *Hin*dIII enzymes, named as *EPIC1*-Luc. WWP-Luc (p21/WAF1 promoter) was a gift from Bert Vogelstein (Addgene plasmid #16451). For plasmid methylation followed by the previous report (DiNardo et al., 2001), briefly, 20 μg of *EPIC1*-Luc were methylated using Methyltransferase (M. SssI, NEB, #M0226S) at 37°C for 12 hr, followed by subsequent inactivation of enzyme at 60°C for 20 min. Mockmethylated mixtures were also performed in the absence of the methylase and Sadenosyl methionine. The methylated and mock-methylated mixtures were purified using QIAprep Spin Miniprep Kit (Qiagen, #27106) and the methylation status of the constructs was determined by HpaII digestion and 2% agarose gel eletrophoresis.

Cells were transiently transfected with un-methylated or methylated *EPIC1*-Luc reporter or a combination of either *EPIC1* siRNA, *MYC* siRNA, or a negative control siRNA with CCNA2-Luc or WWP-Luc constructs using Lipofectamine™ 2000, and β-Gal was used as an internal control. After 48 hr, the luciferase and β-Gal activities were detected as described (Niu et al., 2017) in a Wallac 1420 Victor^2 Microplate Reader (Perkin Elmer). The luciferase activities were normalized to the β-Gal activities. Data were shown as fold change over the control group.

Cell proliferation and cell cycle assay—Cells were seeded at 2,000 cells per well in 96-well culture plates, and MTT assays were performed with a CellTiter 96 Non-Radioactive Cell Proliferation Assay Kit (Promega, #G4100) following the manufacturer's guidelines. The absorbance value was measured at 570 nm using an xMark Microplate Spectrophotometer (Bio-Rad) with a reference wavelength of 630 nm.

For the cell cycle assay, cells were collected, rinsed with PBS, and fixed for a minimum of 2 hr by adding 70% ice-cold ethanol at −20°C. Cells were then sequentially washed once in PBS and BD Pharmingen stain buffer (BD Biosciences, #554656). Cell pellets were resuspended in 0.5 ml of BD Pharmingen PI/RNase staining buffer (BD Biosciences, #550825) and incubated for 15 min at room temperature (RT), and cells were immediately analyzed using an LSRFORTESSA X-20 flow cytometer (BD Biosciences). The data were analyzed with FlowJo software.

Soft agar colony formation assay—For each well, 2 ml of 0.6% NuSieve GTG agarose (Lonza, #50081) in culture medium was plated into 6-well plates as the bottom layer, and the agarose was allowed to solidify at RT. Then, 1 ml of cell mixture containing 10^4 cells in culture medium and a final concentration of 0.35% agarose was carefully plated on top of the bottom layer. The plates were incubated at 37°C and 5% CO_2 until colonies were formed, and cells were fed with 0.5 ml of cell culture medium every other week. After 2–3 weeks, colonies were stained using 0.005% crystal violet in 4% paraformaldehyde solution and counted.

***In vivo* xenograft model—**Briefly, 5- to 6-week-old female athymic nude mice (Charles River) were used for the xenograft model. MCF-7 cells stably expressing shCtrl and sh*EPIC1* were trypsinized and washed twice with sterilized PBS, and then, 0.2 ml of PBS containing 5×10^6 cells was subcutaneously inoculated into the flanks of the mice. Mice were monitored twice every week for tumor growth, and tumor size was measured using a caliper. Tumor volume in mm^3 was calculated using the formula: Tumor volume = $0.5 \times (\text{width})^2 \times \text{length}$. Eight weeks after inoculation, mice were sacrificed in keeping with the policy for the humane treatment of tumor-bearing animals. All animal studies were performed in accordance with the institutional guidelines, and the experiments followed the protocols approved by the Institutional Animal Care and Use Committee (IACUC) of the University of Pittsburgh.

RNA immunoprecipitation (RIP)—RIP was performed as previously described with minor modifications (Tsai et al., 2010). Briefly, cultured cells were collected by trypsinization, washed once with cold PBS, and then treated with 0.3% formaldehyde in PBS for 10 min at 37°C. Then, 1.25 M glycine dissolved in PBS was added to a final concentration of 0.125 M, and the mixture continued to incubate for 5 min at RT. The cells were subsequently washed twice with cold PBS, and the pellets were resuspended in RIPA buffer (50 mM Tris-HCl, pH 7.4, 150 mM NaCl, 1 mM EDTA, 0.1% SDS, 1% NP-40, 0.5% sodium deoxycholate, 0.5 mM DTT, 1 mM PMSF, and 1 × protease inhibitor cocktail (Sigma, #P8340)) and incubated on ice for 30 min with shaking. The cleared lysates were incubated for 4 h at 4°C with the corresponding antibodies. Pellets were washed twice in RIPA buffer, four times in 1 M RIPA buffer (50 mM Tris-HCl, pH 7.4, 1 M NaCl, 1 mM

EDTA, 0.1% SDS, 1% NP-40, and 0.5% sodium deoxycholate), and then twice in RIPA buffer. The pellets were resuspended and treated with RIPA buffer containing proteinase K at 45°C for 45 min. Finally, RNA was isolated with TRIzol reagent.

RNA pull-down assay—Biotin-labeled full-length and truncated fragments of *EPIC1* RNA were transcribed *in vitro* with a Biotin RNA Labeling Mix Kit (Roche, #11685597910) and T7 RNA polymerase (Roche, #10881775001) using the PCR products as a template, treated with RNase-free DNase I (Promega, #M198A), and then isolated with an RNeasy Mini kit. Biotinylated RNA was folded in RNA structure buffer (10 mM Tris-HCl pH 7.0, 0.1 M KCl, 10 mM $MgCl_2$) at 90°C for 2 min, immediately put on ice for ano ther 2 min, and then transferred to RT for 20 min to allow proper RNA secondary structure formation.

Cells were collected by trypsinization and washed twice with sterilized PBS. Cell pellets were resuspended in 2 ml of pre-chilled PBS, 2 ml of nuclear isolation buffer (1.28 M sucrose, 40 mM Tris-HCl pH 7.5, 20 mM $MgCl_2$, and 4% Triton X-100) and 6 ml of sterilized DEPC-treated water and incubated on ice for 20 min with frequent vortexing. Nuclei were pelleted by centrifugation at 2,500 *g* for 15 min, washed once with 1 ml of nuclear isolation buffer, resuspended in RIP buffer (150 mM KCl, 25 mM Tris-HCl pH 7.4, 0.5 mM DTT, 0.5% NP-40, 1 mM PMSF, 1 × Superase-in, and 1 × protease inhibitor cocktail), and sheared on ice using a Dounce homogenizer with 15 to 20 strokes. After 1 mg of the cleared lysate was mixed with folded RNA in RIP buffer and incubated for 1 hr at RT, 60 μl of Dynabeads MyOne Streptavidin C1 magnetic beads (ThermoFisher, #65001) was added to each reaction, and the mixture was incubated for another 1 hr at RT. Beads were washed five times and boiled in 1 × SDS loading buffer, and the retrieved protein was analyzed using western blotting.

The *in vitro* binding assay of biotin-labeled *EPIC1* RNA and MYC protein was performed as previously described (Tsai et al., 2010). Briefly, 0.1 μg of biotinylated RNA was incubated with different amounts of recombinant human MYC protein (Abcam, #ab84132) for 1 hr at RT in 200 μl of binding buffer (50 mM Tris-HCl pH 7.9, 10% glycerol, 100 mM KCl, 5 mM $MgCl_2$, 10 mM β-ME, 0.1% NP-40, 1 mM PMSF, 1 × Superase-in, and 1 × protease inhibitor cocktail). Then, 30 μl of washed streptavidin-conjugated magnetic beads were added to each reaction, and the mixtures were incubated at RT for 30 min. Beads were washed five times and boiled in 1 × SDS loading buffer, and the retrieved protein was analyzed using western blotting.

Chromatin immunoprecipitation (ChIP)—The ChIP assay was performed as previously described (Nelson et al., 2006). Briefly, 1×10^7 cells were cross-linked with a final concentration of 1.42% formaldehyde in growth medium for 15 min at RT, and cross-linking was quenched by the addition of glycine to a final concentration of 125 mM and incubation for 5 min at RT. Cells were rinsed twice with cold PBS, harvested in IP buffer (50 mM pH 7.5 Tris-HCl, 150 mM NaCl, 5 mM EDTA, 0.5% NP-40, and 1% Triton X-100) supplemented with 1 mM PMSF and 1 × protease inhibitor cocktail and sonicated to shear the chromatin to yield DNA fragment sizes of 0.5 to 1 kb. Samples were cleared by centrifuging at 12,000 *g* for 10 min at 4°C and preincubated for 1 hr with 40 μl of protein A/G agarose beads. A portion of the precleared samples was used as input DNA. Then,

approximately 2 μg of MYC antibody or rabbit normal immunoglobulin (IgG) was added to the remainder of the samples and incubated for 1 hr at 4°C, 40 μl of protein A/G aga rose beads (ThermoFisher, #20421) were added, and the mixture was incubated for 4 hr at 4°C. Beads were washed six times with cold IP buffer, and DNA was isolated with 10% Chelex following the suggested protocol; the total input DNA was also isolated. Quantification was performed using real-time PCR with SYBR Green Master Mix. Control IgG and input DNA signal values were used to normalize the values from the MYC ChIP to target genes. The primers for target genes and the negative control are listed in Table S5.

Co-immunoprecipitation (Co-IP), protein isolation and western blotting—Co-IP was performed as following, briefly, cells were collected and lysed in lysis buffer (50 mM Tris-HCl pH 7.5, 150 mM NaCl, 1 mM EDT, 1% Triton X-100, PMSF freshly added to a final concentration of 1mM, and 1x protease inhibitor cocktail). After quantification using a BCA protein assay kit (ThermoFisher, #23225), 1 mg of total protein were used for Co-IP and incubated for overnight with 2 μg of anti-MYC, anti-MAX antibodies, and normal rabbit IgG as a negative IP control, respectively. The mixtures were incubated for another 2–4 hr with protein A/G agarose beads, and then beads were washed at least 4 times, and treated and boiled for 10 min with 1x SDS sample buffer (Bio-Rad, #161–0737).

Cell lysates were also treated with equal volume of 2x SDS sample buffer and resolved by SDS-PAGE under denaturing conditions and transferred onto PVDF membranes (Bio-Rad, #162–0177). The membranes were blocked with 5% non-fat milk (LabScientific, #M0841) in 1x PBST at RT for 2 hr and incubated with primary antibody overnight at 4°C, followed by incubation with horse radish peroxidase-conjugated secondary antibodies for 1 hr at RT. Specific bands were visualized with enhanced chemiluminescence (ECL) substrate (ThermoFisher, #32106) and exposed onto films with an AX 700LE film processor (ALPHATEK).

Supplementary Material

Refer to Web version on PubMed Central for supplementary material.

Acknowledgments

This study was supported by a grant from the Shear Family Foundation (to D. Y.), and a Career Development Award of RPCI-UPCI Ovarian Cancer SPORE (P50 CA159981; to D. Y.), a grant from the Elsa U. Pardee Foundation (to D. Y.). We thank The Center for Simulation and Modeling (SaM) at the University of Pittsburgh for computing assistance. We thank The Center for Biologic Imaging (CBI) at the University of Pittsburgh for imaging assistance. We thank Drs. Nara Lee, Barry Gold, Anil Sood, Wei Zhang, and Ilya Shmulevich for internal critical review.

References

Amati B, Brooks MW, Levy N, Littlewood TD, Evan GI, Land H. Oncogenic activity of the c-Myc protein requires dimerization with Max. Cell. 1993; 72:233–245. [PubMed: 8425220]

Amin V, Harris RA, Onuchic V, Jackson AR, Charnecki T, Paithankar S, Lakshmi Subramanian S, Riehle K, Coarfa C, Milosavljevic A. Epigenomic footprints across 111 reference epigenomes reveal tissue-specific epigenetic regulation of lincRNAs. Nat Commun. 2015; 6:6370. [PubMed: 25691256]

Anders S, Huber W. Differential expression analysis for sequence count data. Genome Biol. 2010; 11:R106. [PubMed: 20979621]

Barretina J, Caponigro G, Stransky N, Venkatesan K, Margolin AA, Kim S, Wilson CJ, Lehar J, Kryukov GV, Sonkin D, et al. The Cancer Cell Line Encyclopedia enables predictive modelling of anticancer drug sensitivity. Nature. 2012; 483:603–607. [PubMed: 22460905]

Batista PJ, Chang HY. Long noncoding RNAs: cellular address codes in development and disease. Cell. 2013; 152:1298–1307. [PubMed: 23498938]

Baylin SB, Hoppener JW, de Bustros A, Steenbergh PH, Lips CJ, Nelkin BD. DNA methylation patterns of the calcitonin gene in human lung cancers and lymphomas. Cancer Res. 1986; 46:2917–2922. [PubMed: 3009002]

Benjamini Y, Hochberg Y. Controlling the false discovery rate: a practical and powerful approach to multiple testing. Royal Statistical Society Series B. 1995; 57:289.

Blackwood EM, Eisenman RN. Max: a helix-loop-helix zipper protein that forms a sequence-specific DNA-binding complex with Myc. Science. 1991; 251:1211–1217. [PubMed: 2006410]

Cawley S, Bekiranov S, Ng HH, Kapranov P, Sekinger EA, Kampa D, Piccolboni A, Sementchenko V, Cheng J, Williams AJ, et al. Unbiased mapping of transcription factor binding sites along human chromosomes 21 and 22 points to widespread regulation of noncoding RNAs. Cell. 2004; 116:499–509. [PubMed: 14980218]

Consortium EP. An integrated encyclopedia of DNA elements in the human genome. Nature. 2012; 489:57–74. [PubMed: 22955616]

Dang CV. MYC on the path to cancer. Cell. 2012; 149:22–35. [PubMed: 22464321]

Di Cello F, Cope L, Li H, Jeschke J, Wang W, Baylin SB, Zahnow CA. Methylation of the claudin 1 promoter is associated with loss of expression in estrogen receptor positive breast cancer. PLoS One. 2013; 8:e68630. [PubMed: 23844228]

DiNardo DN, Butcher DT, Robinson DP, Archer TK, Rodenhiser DI. Functional analysis of CpG methylation in the BRCA1 promoter region. Oncogene. 2001; 20:5331–5340. [PubMed: 11536045]

Doose G, Haake A, Bernhart SH, Lopez C, Duggimpudi S, Wojciech F, Bergmann AK, Borkhardt A, Burkhardt B, Claviez A, et al. MINCR is a MYC-induced lncRNA able to modulate MYC's transcriptional network in Burkitt lymphoma cells. Proc Natl Acad Sci U S A. 2015; 112:E5261–5270. [PubMed: 26351698]

Du Z, Fei T, Verhaak RG, Su Z, Zhang Y, Brown M, Chen Y, Liu XS. Integrative genomic analyses reveal clinically relevant long noncoding RNAs in human cancer. Nat Struct Mol Biol. 2013; 20:908–913. [PubMed: 23728290]

Du Z, Sun T, Hacisuleyman E, Fei T, Wang X, Brown M, Rinn JL, Lee MG, Chen Y, Kantoff PW, Liu XS. Integrative analyses reveal a long noncoding RNA-mediated sponge regulatory network in prostate cancer. Nat Commun. 2016; 7:10982. [PubMed: 26975529]

Engel JR, Smallwood A, Harper A, Higgins MJ, Oshimura M, Reik W, Schofield PN, Maher ER. Epigenotype-phenotype correlations in Beckwith-Wiedemann syndrome. J Med Genet. 2000; 37:921–926. [PubMed: 11106355]

Fernandez PC, Frank SR, Wang L, Schroeder M, Liu S, Greene J, Cocito A, Amati B. Genomic targets of the human c-Myc protein. Genes Dev. 2003; 17:1115–1129. [PubMed: 12695333]

Gartel AL, Radhakrishnan SK. Lost in transcription: p21 repression, mechanisms, and consequences. Cancer Res. 2005; 65:3980–3985. [PubMed: 15899785]

Gartel AL, Ye X, Goufman E, Shianov P, Hay N, Najmabadi F, Tyner AL. Myc represses the p21(WAF1/CIP1) promoter and interacts with Sp1/Sp3. Proc Natl Acad Sci U S A. 2001; 98:4510–4515. [PubMed: 11274368]

Guo H, Ahmed M, Zhang F, Yao CQ, Li S, Liang Y, Hua J, Soares F, Sun Y, Langstein J, et al. Modulation of long noncoding RNAs by risk SNPs underlying genetic predispositions to prostate cancer. Nat Genet. 2016

Gupta RA, Shah N, Wang KC, Kim J, Horlings HM, Wong DJ, Tsai MC, Hung T, Argani P, Rinn JL, et al. Long non-coding RNA HOTAIR reprograms chromatin state to promote cancer metastasis. Nature. 2010; 464:1071–1076. [PubMed: 20393566]

Guttman M, Amit I, Garber M, French C, Lin MF, Feldser D, Huarte M, Zuk O, Carey BW, Cassady JP, et al. Chromatin signature reveals over a thousand highly conserved large non-coding RNAs in mammals. Nature. 2009; 458:223–227. [PubMed: 19182780]

Hancock AL, Brown KW, Moorwood K, Moon H, Holmgren C, Mardikar SH, Dallosso AR, Klenova E, Loukinov D, Ohlsson R, et al. A CTCF-binding silencer regulates the imprinted genes AWT1 and WT1-AS and exhibits sequential epigenetic defects during Wilms' tumourigenesis. Hum Mol Genet. 2007; 16:343–354. [PubMed: 17210670]

Hu X, Feng Y, Zhang D, Zhao SD, Hu Z, Greshock J, Zhang Y, Yang L, Zhong X, Wang LP, et al. A functional genomic approach identifies FAL1 as an oncogenic long noncoding RNA that associates with BMI1 and represses p21 expression in cancer. Cancer Cell. 2014; 26:344–357. [PubMed: 25203321]

Hung CL, Wang LY, Yu YL, Chen HW, Srivastava S, Petrovics G, Kung HJ. A long noncoding RNA connects c-Myc to tumor metabolism. Proc Natl Acad Sci U S A. 2014; 111:18697–18702. [PubMed: 25512540]

Iorio F, Knijnenburg TA, Vis DJ, Bignell GR, Menden MP, Schubert M, Aben N, Goncalves E, Barthorpe S, Lightfoot H, et al. A Landscape of Pharmacogenomic Interactions in Cancer. Cell. 2016; 166:740–754. [PubMed: 27397505]

Irizarry RA, Ladd-Acosta C, Wen B, Wu Z, Montano C, Onyango P, Cui H, Gabo K, Rongione M, Webster M, et al. The human colon cancer methylome shows similar hypo- and hypermethylation at conserved tissue-specific CpG island shores. Nat Genet. 2009; 41:178–186. [PubMed: 19151715]

Iyer MK, Niknafs YS, Malik R, Singhal U, Sahu A, Hosono Y, Barrette TR, Prensner JR, Evans JR, Zhao S, et al. The landscape of long noncoding RNAs in the human transcriptome. Nat Genet. 2015; 47:199–208. [PubMed: 25599403]

Izumi H, Molander C, Penn LZ, Ishisaki A, Kohno K, Funa K. Mechanism for the transcriptional repression by c-Myc on PDGF beta-receptor. J Cell Sci. 2001; 114:1533–1544. [PubMed: 11282029]

Jones PA, Baylin SB. The fundamental role of epigenetic events in cancer. Nat Rev Genet. 2002; 3:415–428. [PubMed: 12042769]

Kress TR, Sabo A, Amati B. MYC: connecting selective transcriptional control to global RNA production. Nat Rev Cancer. 2015; 15:593–607. [PubMed: 26383138]

Lee BK, Bhinge AA, Battenhouse A, McDaniell RM, Liu Z, Song L, Ni Y, Birney E, Lieb JD, Furey TS, et al. Cell-type specific and combinatorial usage of diverse transcription factors revealed by genome-wide binding studies in multiple human cells. Genome Res. 2012; 22:9–24. [PubMed: 22090374]

Lehmann BD, Bauer JA, Chen X, Sanders ME, Chakravarthy AB, Shyr Y, Pietenpol JA. Identification of human triple-negative breast cancer subtypes and preclinical models for selection of targeted therapies. J Clin Invest. 2011; 121:2750–2767. [PubMed: 21633166]

Leucci E, Vendramin R, Spinazzi M, Laurette P, Fiers M, Wouters J, Radaelli E, Eyckerman S, Leonelli C, Vanderheyden K, et al. Melanoma addiction to the long non-coding RNA SAMMSON. Nature. 2016; 531:518–522. [PubMed: 27008969]

Li B, Ruotti V, Stewart RM, Thomson JA, Dewey CN. RNA-Seq gene expression estimation with read mapping uncertainty. Bioinformatics. 2010; 26:493–500. [PubMed: 20022975]

Li H, Chiappinelli KB, Guzzetta AA, Easwaran H, Yen RW, Vatapalli R, Topper MJ, Luo J, Connolly RM, Azad NS, et al. Immune regulation by low doses of the DNA methyltransferase inhibitor 5-azacitidine in common human epithelial cancers. Oncotarget. 2014; 5:587–598. [PubMed: 24583822]

Li JP, Liu LH, Li J, Chen Y, Jiang XW, Ouyang YR, Liu YQ, Zhong H, Li H, Xiao T. Microarray expression profile of long noncoding RNAs in human osteosarcoma. Biochem Biophys Res Commun. 2013; 433:200–206. [PubMed: 23466354]

Li Z, Van Calcar S, Qu C, Cavenee WK, Zhang MQ, Ren B. A global transcriptional regulatory role for c-Myc in Burkitt's lymphoma cells. Proc Natl Acad Sci U S A. 2003; 100:8164–8169. [PubMed: 12808131]

Luscher B. Function and regulation of the transcription factors of the Myc/Max/Mad network. Gene. 2001; 277:1–14. [PubMed: 11602341]

Mei S, Qin Q, Wu Q, Sun H, Zheng R, Zang C, Zhu M, Wu J, Shi X, Taing L, et al. Cistrome Data Browser: a data portal for ChIP-Seq and chromatin accessibility data in human and mouse. Nucleic Acids Res. 2017; 45:D658–D662. [PubMed: 27789702]

Nelson JD, Denisenko O, Bomsztyk K. Protocol for the fast chromatin immunoprecipitation (ChIP) method. Nat Protoc. 2006; 1:179–185. [PubMed: 17406230]

Niu Y, Xu M, Slagle BL, Huang H, Li S, Guo GL, Shi G, Qin W, Xie W. Farnesoid X receptor ablation sensitizes mice to hepatitis b virus X protein-induced hepatocarcinogenesis. Hepatology. 2017; 65:893–906. [PubMed: 28102638]

Noushmehr H, Weisenberger DJ, Diefes K, Phillips HS, Pujara K, Berman BP, Pan F, Pelloski CE, Sulman EP, Bhat KP, et al. Identification of a CpG island methylator phenotype that defines a distinct subgroup of glioma. Cancer Cell. 2010; 17:510–522. [PubMed: 20399149]

Peukert K, Staller P, Schneider A, Carmichael G, Hanel F, Eilers M. An alternative pathway for gene regulation by Myc. EMBO J. 1997; 16:5672–5686. [PubMed: 9312026]

Prensner JR, Chinnaiyan AM. The emergence of lncRNAs in cancer biology. Cancer Discov. 2011; 1:391–407. [PubMed: 22096659]

Roy AL, Carruthers C, Gutjahr T, Roeder RG. Direct role for Myc in transcription initiation mediated by interactions with TFII-I. Nature. 1993; 365:359–361. [PubMed: 8377829]

Ruan W, Wang P, Feng S, Xue Y, Li Y. Long non-coding RNA small nucleolar RNA host gene 12 (SNHG12) promotes cell proliferation and migration by upregulating angiomotin gene expression in human osteosarcoma cells. Tumour Biol. 2016; 37:4065–4073. [PubMed: 26486328]

Sanchez Y, Segura V, Marin-Bejar O, Athie A, Marchese FP, Gonzalez J, Bujanda L, Guo S, Matheu A, Huarte M. Genome-wide analysis of the human p53 transcriptional network unveils a lncRNA tumour suppressor signature. Nat Commun. 2014; 5:5812. [PubMed: 25524025]

Schmitt AM, Chang HY. Long Noncoding RNAs in Cancer Pathways. Cancer Cell. 2016; 29:452–463. [PubMed: 27070700]

Schmitt AM, Garcia JT, Hung T, Flynn RA, Shen Y, Qu K, Payumo AY, Peresda-Silva A, Broz DK, Baum R, et al. An inducible long noncoding RNA amplifies DNA damage signaling. Nat Genet. 2016; 48:1370–1376. [PubMed: 27668660]

Scott RH, Douglas J, Baskcomb L, Huxter N, Barker K, Hanks S, Craft A, Gerrard M, Kohler JA, Levitt GA, et al. Constitutional 11p15 abnormalities, including heritable imprinting center mutations, cause nonsyndromic Wilms tumor. Nat Genet. 2008; 40:1329–1334. [PubMed: 18836444]

Shen H, Laird PW. Interplay between the cancer genome and epigenome. Cell. 2013; 153:38–55. [PubMed: 23540689]

Shlyueva D, Stampfel G, Stark A. Transcriptional enhancers: from properties to genome-wide predictions. Nat Rev Genet. 2014; 15:272–286. [PubMed: 24614317]

Shrivastava A, Saleque S, Kalpana GV, Artandi S, Goff SP, Calame K. Inhibition of transcriptional regulator Yin-Yang-1 by association with c-Myc. Science. 1993; 262:1889–1892. [PubMed: 8266081]

Subramanian A, Tamayo P, Mootha VK, Mukherjee S, Ebert BL, Gillette MA, Paulovich A, Pomeroy SL, Golub TR, Lander ES, Mesirov JP. Gene set enrichment analysis: a knowledge-based approach for interpreting genome-wide expression profiles. Proc Natl Acad Sci U S A. 2005; 102:15545–15550. [PubMed: 16199517]

Tsai MC, Manor O, Wan Y, Mosammaparast N, Wang JK, Lan F, Shi Y, Segal E, Chang HY. Long noncoding RNA as modular scaffold of histone modification complexes. Science. 2010; 329:689–693. [PubMed: 20616235]

Tseng YY, Moriarity BS, Gong W, Akiyama R, Tiwari A, Kawakami H, Ronning P, Reuland B, Guenther K, Beadnell TC, et al. PVT1 dependence in cancer with MYC copy-number increase. Nature. 2014; 512:82–86. [PubMed: 25043044]

Vogelstein B, Papadopoulos N, Velculescu VE, Zhou S, Diaz LA Jr, Kinzler KW. Cancer genome landscapes. Science. 2013; 339:1546–1558. [PubMed: 23539594]

von der Lehr N, Johansson S, Wu S, Bahram F, Castell A, Cetinkaya C, Hydbring P, Weidung I, Nakayama K, Nakayama KI, et al. The F-box protein Skp2 participates in c-Myc proteosomal degradation and acts as a cofactor for c-Myc-regulated transcription. Mol Cell. 2003; 11:1189–1200. [PubMed: 12769844]

Wagner GP, Kin K, Lynch VJ. Measurement of mRNA abundance using RNA-seq data: RPKM measure is inconsistent among samples. Theory Biosci. 2012; 131:281–285. [PubMed: 22872506]

Wijnen M, Alders M, Zwaan CM, Wagner A, van den Heuvel-Eibrink MM. KCNQ1OT1 hypomethylation: a novel disguised genetic predisposition in sporadic pediatric adrenocortical tumors? Pediatr Blood Cancer. 2012; 59:565–566. [PubMed: 22610651]

Wu SC, Kallin EM, Zhang Y. Role of H3K27 methylation in the regulation of lncRNA expression. Cell Res. 2010; 20:1109–1116. [PubMed: 20680032]

Xiang JF, Yin QF, Chen T, Zhang Y, Zhang XO, Wu Z, Zhang S, Wang HB, Ge J, Lu X, et al. Human colorectal cancer-specific CCAT1-L lncRNA regulates long-range chromatin interactions at the MYC locus. Cell Res. 2014; 24:513–531. [PubMed: 24662484]

Yan X, Hu Z, Feng Y, Hu X, Yuan J, Zhao SD, Zhang Y, Yang L, Shan W, He Q, et al. Comprehensive Genomic Characterization of Long Non-coding RNAs across Human Cancers. Cancer Cell. 2015; 28:529–540. [PubMed: 26461095]

Yang F, Xue X, Zheng L, Bi J, Zhou Y, Zhi K, Gu Y, Fang G. Long non-coding RNA GHET1 promotes gastric carcinoma cell proliferation by increasing c-Myc mRNA stability. FEBS J. 2014; 281:802–813. [PubMed: 24397586]

Zeller KI, Zhao X, Lee CW, Chiu KP, Yao F, Yustein JT, Ooi HS, Orlov YL, Shahab A, Yong HC, et al. Global mapping of c-Myc binding sites and target gene networks in human B cells. Proc Natl Acad Sci U S A. 2006; 103:17834–17839. [PubMed: 17093053]

Zhou Y, Zhang X, Klibanski A. MEG3 noncoding RNA: a tumor suppressor. J Mol Endocrinol. 2012; 48:R45–53. [PubMed: 22393162]

Zhu S, Li W, Liu J, Chen CH, Liao Q, Xu P, Xu H, Xiao T, Cao Z, Peng J, et al. Genome-scale deletion screening of human long non-coding RNAs using a paired-guide RNA CRISPR-Cas9 library. Nat Biotechnol. 2016; 34:1279–1286. [PubMed: 27798563]

Appendix

Secondary author list

Amy Blum, Samantha J. Caesar-Johnson, John A. Demchok, Ina Felau, Melpomeni Kasapi, Martin L. Ferguson, Carolyn M. Hutter, Heidi J. Sofia, Roy Tarnuzzer, Peggy Wang, Zhining Wang, Liming Yang, Jean C. Zenklusen, Jiashan (Julia) Zhang, Sudha Chudamani, Jia Liu, Laxmi Lolla, Rashi Naresh, Todd Pihl, Qiang Sun, Yunhu Wan, Ye Wu, Juok Cho, Timothy DeFreitas, Scott Frazer, Nils Gehlenborg, Gad Getz, David I. Heiman, Jaegil Kim, Michael S. Lawrence, Pei Lin, Sam Meier, Michael S. Noble, Gordon Saksena, Doug Voet, Hailei Zhang, Brady Bernard, Nyasha Chambwe, Varsha Dhankani, Theo Knijnenburg, Roger Kramer, Kalle Leinonen, Yuexin Liu, Michael Miller, Sheila Reynolds, Ilya Shmulevich, Vesteinn Thorsson, Wei Zhang, Rehan Akbani, Bradley M. Broom, Apurva M. Hegde, Zhenlin Ju, Rupa S. Kanchi, Anil Korkut, Jun Li, Han Liang, Shiyun Ling, Wenbin Liu, Yiling Lu, Gordon B. Mills, Kwok-Shing Ng, Arvind Rao, Michael Ryan, Jing Wang, John N. Weinstein, Jiexin Zhang, Adam Abeshouse, Joshua Armenia, Debyani Chakravarty, Walid K. Chatila, Ino de Bruijn, Jianjiong Gao, Benjamin E. Gross, Zachary J. Heins, Ritika Kundra, Konnor La, Marc Ladanyi, Augustin Luna, Moriah G. Nissan, Angelica Ochoa, Sarah M. Phillips, Ed Reznik, Francisco Sanchez-Vega, Chris Sander, Nikolaus Schultz, Robert Sheridan, S. Onur Sumer, Yichao Sun, Barry S. Taylor, Jioajiao Wang, Hongxin Zhang, Pavana Anur, Myron Peto, Paul Spellman, Christopher Benz, Joshua M. Stuart,

Christopher K. Wong, Christina Yau, D. Neil Hayes, Joel S. Parker, Matthew D. Wilkerson, Adrian Ally, Miruna Balasundaram, Reanne Bowlby, Denise Brooks, Rebecca Carlsen, Eric Chuah, Noreen Dhalla, Robert Holt, Steven J.M. Jones, Katayoon Kasaian, Darlene Lee, Yussanne Ma, Marco A. Marra, Michael Mayo, Richard A. Moore, Andrew J. Mungall, Karen Mungall, A. Gordon Robertson, Sara Sadeghi, Jacqueline E. Schein, Payal Sipahimalani, Angela Tam, Nina Thiessen, Kane Tse, Tina Wong, Ashton C. Berger, Rameen Beroukhim, Andrew D. Cherniack, Carrie Cibulskis, Stacey B. Gabriel, Galen F. Gao, Gavin Ha, Matthew Meyerson, Steven E. Schumacher, Juliann Shih, Melanie H. Kucherlapati, Raju S. Kucherlapati, Stephen Baylin, Leslie Cope, Ludmila Danilova, Moiz S. Bootwalla, Phillip H. Lai, Dennis T. Maglinte, David J. Van Den Berg, Daniel J. Weisenberger, J. Todd Auman, Saianand Balu, Tom Bodenheimer, Cheng Fan, Katherine A. Hoadley, Alan P. Hoyle, Stuart R. Jefferys, Corbin D. Jones, Shaowu Meng, Piotr A. Mieczkowski, Lisle E. Mose, Amy H. Perou, Charles M. Perou, Jeffrey Roach, Yan Shi, Janae V. Simons, Tara Skelly, Matthew G. Soloway, Donghui Tan, Umadevi Veluvolu, Huihui Fan, Toshinori Hinoue, Peter W. Laird, Hui Shen, Wanding Zhou, Michelle Bellair, Kyle Chang, Kyle Covington, Chad J. Creighton, Huyen Dinh, HarshaVardhan Doddapaneni, Lawrence A. Donehower, Jennifer Drummond, Richard A. Gibbs, Robert Glenn, Walker Hale, Yi Han, Jianhong Hu, Viktoriya Korchina, Sandra Lee, Lora Lewis, Wei Li, Xiuping Liu, Margaret Morgan, Donna Morton, Donna Muzny, Jireh Santibanez, Margi Sheth, Eve Shinbrot, Linghua Wang, Min Wang, David A. Wheeler, Liu Xi, Fengmei Zhao, Julian Hess, Elizabeth L. Appelbaum, Matthew Bailey, Matthew G. Cordes, Li Ding, Catrina C. Fronick, Lucinda A. Fulton, Robert S. Fulton, Cyriac Kandoth, Elaine R. Mardis, Michael D. McLellan, Christopher A. Miller, Heather K. Schmidt, Richard K. Wilson, Daniel Crain, Erin Curley, Johanna Gardner, Kevin Lau, David Mallery, Scott Morris, Joseph Paulauskis, Robert Penny, Candace Shelton, Troy Shelton, Mark Sherman, Eric Thompson, Peggy Yena, Jay Bowen, Julie M. Gastier-Foster, Mark Gerken, Kristen M. Leraas, Tara M. Lichtenberg, Nilsa C. Ramirez, Lisa Wise, Erik Zmuda, Niall Corcoran, Tony Costello, Christopher Hovens, Andre L. Carvalho, Ana C. de Carvalho, José H. Fregnani, Adhemar Longatto-Filho, Rui M. Reis, Cristovam Scapulatempo-Neto, Henrique C.S. Silveira, Daniel O. Vidal, Andrew Burnette, Jennifer Eschbacher, Beth Hermes, Ardene Noss, Rosy Singh, Matthew L. Anderson, Patricia D. Castro, Michael Ittmann, David Huntsman, Bernard Kohl, Xuan Le, Richard Thorp, Chris Andry, Elizabeth R. Duffy, Vladimir Lyadov, Oxana Paklina, Galiya Setdikova, Alexey Shabunin, Mikhail Tavobilov, Christopher McPherson, Ronald Warnick, Ross Berkowitz, Daniel Cramer, Colleen Feltmate, Neil Horowitz, Adam Kibel, Michael Muto, Chandrajit P. Raut, Andrei Malykh, Jill S. Barnholtz-Sloan, Wendi Barrett, Karen Devine, Jordonna Fulop, Quinn T. Ostrom, Kristen Shimmel, Yingli Wolinsky, Andrew E. Sloan, Agostino De Rose, Felice Giuliante, Marc Goodman, Beth Y. Karlan, Curt H. Hagedorn, John Eckman, Jodi Harr, Jerome Myers, Kelinda Tucker, Leigh Anne Zach, Brenda Deyarmin, Hai Hu, Leonid Kvecher, Caroline Larson, Richard J. Mural, Stella Somiari, Ales Vicha, Tomas Zelinka, Joseph Bennett, Mary Iacocca, Brenda Rabeno, Patricia Swanson, Mathieu Latour, Louis Lacombe, Bernard Têtu, Alain Bergeron, Mary McGraw, Susan M. Staugaitis, John Chabot, Hanina Hibshoosh, Antonia Sepulveda, Tao Su, Timothy Wang, Olga Potapova, Olga Voronina, Laurence Desjardins, Odette Mariani, Sergio Roman-Roman, Xavier Sastre, Marc-Henri Stern, Feixiong Cheng, Sabina Signoretti, Andrew Berchuck, Darell Bigner, Eric Lipp, Jeffrey

Marks, Shannon McCall, Roger McLendon, Angeles Secord, Alexis Sharp, Madhusmita Behera, Daniel J. Brat, Amy Chen, Keith Delman, Seth Force, Fadlo Khuri, Kelly Magliocca, Shishir Maithel, Jeffrey J. Olson, Taofeek Owonikoko, Alan Pickens, Suresh Ramalingam, Dong M. Shin, Gabriel Sica, Erwin G. Van Meir, Hongzheng Zhang, Wil Eijckenboom, Ad Gillis, Esther Korpershoek, Leendert Looijenga, Wolter Oosterhuis, Hans Stoop, Kim E. van Kessel, Ellen C. Zwarthoff, Chiara Calatozzolo, Lucia Cuppini, Stefania Cuzzubbo, Francesco DiMeco, Gaetano Finocchiaro, Luca Mattei, Alessandro Perin, Bianca Pollo, Chu Chen, John Houck, Pawadee Lohavanichbutr, Arndt Hartmann, Christine Stoehr, Robert Stoehr, Helge Taubert, Sven Wach, Bernd Wullich, Witold Kycler, Dawid Murawa, Maciej Wiznerowicz, Ki Chung, W. Jeffrey Edenfield, Julie Martin, Eric Baudin, Glenn Bubley, Raphael Bueno, Assunta De Rienzo, William G. Richards, Steven Kalkanis, Tom Mikkelsen, Houtan Noushmehr, Lisa Scarpace, Nicolas Girard, Marta Aymerich, Elias Campo, Eva Giné, Armando López Guillermo, Nguyen Van Bang, Phan Thi Hanh, Bui Duc Phu, Yufang Tang, Howard Colman, Kimberley Evason, Peter R. Dottino, John A. Martignetti, Hani Gabra, Hartmut Juhl, Teniola Akeredolu, Serghei Stepa, Dave Hoon, Keunsoo Ahn, Koo Jeong Kang, Felix Beuschlein, Anne Breggia, Michael Birrer, Debra Bell, Mitesh Borad, Alan H. Bryce, Erik Castle, Vishal Chandan, John Cheville, John A. Copland, Michael Farnell, Thomas Flotte, Nasra Giama, Thai Ho, Michael Kendrick, Jean-Pierre Kocher, Karla Kopp, Catherine Moser, David Nagorney, Daniel O’Brien, Brian Patrick O’Neill, Tushar Patel, Gloria Petersen, Florencia Que, Michael Rivera, Lewis Roberts, Robert Smallridge, Thomas Smyrk, Melissa Stanton, R. Houston Thompson, Michael Torbenson, Ju Dong Yang, Lizhi Zhang, Fadi Brimo, Jaffer A. Ajani, Ana Maria Angulo Gonzalez, Carmen Behrens, Jolanta Bondaruk, Russell Broaddus, Bogdan Czerniak, Bita Esmaeli, Junya Fujimoto, Jeffrey Gershenwald, Charles Guo, Alexander J. Lazar, Christopher Logothetis, Funda Meric-Bernstam, Cesar Moran, Lois Ramondetta, David Rice, Anil Sood, Pheroze Tamboli, Timothy Thompson, Patricia Troncoso, Anne Tsao, Ignacio Wistuba, Candace Carter, Lauren Haydu, Peter Hersey, Valerie Jakrot, Hojabr Kakavand, Richard Kefford, Kenneth Lee, Georgina Long, Graham Mann, Michael Quinn, Robyn Saw, Richard Scolyer, Kerwin Shannon, Andrew Spillane, Jonathan Stretch, Maria Synott, John Thompson, James Wilmott, Hikmat Al-Ahmadie, Timothy A. Chan, Ronald Ghossein, Anuradha Gopalan, Douglas A. Levine, Victor Reuter, Samuel Singer, Bhuvanesh Singh, Nguyen Viet Tien, Thomas Broudy, Cyrus Mirsaidi, Praveen Nair, Paul Drwiega, Judy Miller, Jennifer Smith, Howard Zaren, Joong-Won Park, Nguyen Phi Hung, Electron Kebebew, W. Marston Linehan, Adam R. Metwalli, Karel Pacak, Peter A. Pinto, Mark Schiffman, Laura S. Schmidt, Cathy D. Vocke, Nicolas Wentzensen, Robert Worrell, Hannah Yang, Marc Moncrieff, Chandra Goparaju, Jonathan Melamed, Harvey Pass, Natalia Botnariuc, Irina Caraman, Mircea Cernat, Inga Chemencedji, Adrian Clipca, Serghei Doruc, Ghenadie Gorincioi, Sergiu Mura, Maria Pirtac, Irina Stancul, Diana Tcaciuc, Monique Albert, Iakovina Alexopoulou, Angel Arnaout, John Bartlett, Jay Engel, Sebastien Gilbert, Jeremy Parfitt, Harman Sekhon, George Thomas, Doris M. Rassl, Robert C. Rintoul, Carlo Bifulco, Raina Tamakawa, Walter Urba, Nicholas Hayward, Henri Timmers, Anna Antenucci, Francesco Facciolo, Gianluca Grazi, Mirella Marino, Roberta Merola, Ronald de Krijger, Anne- Paule Gimenez-Roqueplo, Alain Piché, Simone Chevalier, Ginette McKercher, Kivanc Birsoy, Gene Barnett, Cathy Brewer, Carol Farver, Theresa Naska, Nathan A. Pennell, Daniel Raymond, Cathy Schilero, Kathy Smolenski, Felicia Williams,

Carl Morrison, Jeffrey A. Borgia, Michael J. Liptay, Mark Pool, Christopher W. Seder, Kerstin Junker, Larsson Omberg, Mikhail Dinkin, George Manikhas, Domenico Alvaro, Maria Consiglia Bragazzi, Vincenzo Cardinale, Guido Carpino, Eugenio Gaudio, David Chesla, Sandra Cottingham, Michael Dubina, Fedor Moiseenko, Renumathy Dhanasekaran, Karl-Friedrich Becker, Klaus-Peter Janssen, Julia Slotta-Huspenina, Mohamed H. Abdel-Rahman, Dina Aziz, Sue Bell, Colleen M. Cebulla, Amy Davis, Rebecca Duell, J. Bradley Elder, Joe Hilty, Bahavna Kumar, James Lang, Norman L. Lehman, Randy Mandt, Phuong Nguyen, Robert Pilarski, Karan Rai, Lynn Schoenfield, Kelly Senecal, Paul Wakely, Paul Hansen, Ronald Lechan, James Powers, Arthur Tischler, William E. Grizzle, Katherine C. Sexton, Alison Kastl, Joel Henderson, Sima Porten, Jens Waldmann, Martin Fassnacht, Sylvia L. Asa, Dirk Schadendorf, Marta Couce, Markus Graefen, Hartwig Huland, Guido Sauter, Thorsten Schlomm, Ronald Simon, Pierre Tennstedt, Oluwole Olabode, Mark Nelson, Oliver Bathe, Peter R. Carroll, June M. Chan, Philip Disaia, Pat Glenn, Robin K. Kelley, Charles N. Landen, Joanna Phillips, Michael Prados, Jeff Simko, Jeffry Simko, Karen Smith-McCune, Scott VandenBerg, Kevin Roggin, Ashley Fehrenbach, Ady Kendler, Suzanne Sifri, Ruth Steele, Antonio Jimeno, Francis Carey, Ian Forgie, Massimo Mannelli, Michael Carney, Brenda Hernandez, Benito Campos, Christel Herold-Mende, Christin Jungk, Andreas Unterberg, Andreas von Deimling, Aaron Bossler, Joseph Galbraith, Laura Jacobus, Michael Knudson, Tina Knutson, Deqin Ma, Mohammed Milhem, Rita Sigmund, Andrew K. Godwin, Rashna Madan, Howard G. Rosenthal, Clement Adebamowo, Sally N. Adebamowo, Alex Boussioutas, David Beer, Thomas Giordano, Anne-Marie Mes-Masson, Fred Saad, Therese Bocklage, Lisa Landrum, Robert Mannel, Kathleen Moore, Katherine Moxley, Russel Postier, Joan Walker, Rosemary Zuna, Michael Feldman, Federico Valdivieso, Rajiv Dhir, James Luketich, Edna M. Mora Pinero, Mario Quintero-Aguilo, Carlos Gilberto Carlotti, Jr., Jose Sebastião Dos Santos, Rafael Kemp, Ajith Sankarankuty, Daniela Tirapelli, James Catto, Kathy Agnew, Elizabeth Swisher, Jenette Creaney, Bruce Robinson, Carl Simon Shelley, Eryn M. Godwin, Sara Kendall, Cassaundra Shipman, Carol Bradford, Thomas Carey, Andrea Haddad, Jeffey Moyer, Lisa Peterson, Mark Prince, Laura Rozek, Gregory Wolf, Rayleen Bowman, Kwun M. Fong, Ian Yang, Robert Korst, W. Kimryn Rathmell, J. Leigh Fantacone-Campbell, Jeffrey A. Hooke, Albert J. Kovatich, Craig D. Shriver, John DiPersio, Bettina Drake, Ramaswamy Govindan, Sharon Heath, Timothy Ley, Brian Van Tine, Peter Westervelt, Mark A. Rubin, Jung Il Lee, Natália D. Aredes, Armaz Mariamidze, Anant Agrawal, Jaeil Ahn, Jordan Aissiou, Dimitris Anastassiou, Jesper B. Andersen, Jurandyr M. Andrade, Marco Antoniotti, Jon C. Aster, Donald Ayer, Matthew H. Bailey, Rohan Bareja, Adam J. Bass, Azfar Basunia, Oliver F. Bathe, Rebecca Batiste, Oliver Bear Don't Walk, Davide Bedognetti, Gloria Bertoli, Denis Bertrand, Bhavneet Bhinder, Gianluca Bontempi, Dante Bortone, Donald P. Bottaro, Paul Boutros, Kevin Brennan, Chaya Brodie, Scott Brown, Susan Bullman, Silvia Buonamici, Tomasz Burzykowski, Lauren Averett Byers, Fernando Camargo, Joshua D. Campbell, Francisco J. Candido dos Reis, Shaolong Cao, Maria Cardenas, Helio H.A. Carrara, Isabella Castiglioni, Anavaleria Castro, Claudia Cava, Michele Ceccarelli, Shengjie Chai, Kridsadakorn Chaichoompu, Matthew T. Chang, Han Chen, Haoran Chen, Hu Chen, Jian Chen, Jianhong Chen, Ken Chen, Ting-Wen Chen, Zhong Chen, Zhongyuan Chen, Hui Cheng, Hua-Sheng Chiu, Cai Chunhui, Giovanni Ciriello, Cristian Coarfa, Antonio Colaprico, Lee Cooper, Daniel Cui Zhou, Aedin C. Culhane, Christina Curtis, Patrycja Czerwińska, Aditya

Deshpande, Lixia Diao, Michael Dill, Di Du, Charles G. Eberhart, James A. Eddy, Robert N. Eisenman, Mohammed Elanbari, Olivier Elemento, Kyle Ellrott, Manel Esteller, Farshad Farshidfar, Bin Feng, Camila Ferreira de Souza, Esla R. Flores, Steven Foltz, Mitchell T. Frederick, Qingsong Gao, Carl M. Gay, Zhongqi Ge, Andrew J. Gentles, Olivier Gevaert, David L. Gibbs, Adam Godzik, Abel Gonzalez-Perez, Marc T. Goodman, Dmitry A. Gordenin, Carla Grandori, Alex Graudenzi, Casey Greene, Justin Guinney, Margaret L. Gulley, Preethi H. Gunaratne, A. Ari Hakimi, Peter Hammerman, Leng Han, Holger Heyn, Le Hou, Donglei Hu, Kuan-lin Huang, Joerg Huelsken, Scott Huntsman, Peter Hurlin, Matthias Hüser, Antonio Iavarone, Marcin Imielinski, Mirazul Islam, Jacek Jassem, Peilin Jia, Cigall Kadoch, Andre Kahles, Benny Kaipparettu, Bozena Kaminska, Havish Kantheti, Rachel Karchin, Mostafa Karimi, Ekta Khurana, Pora Kim, Leszek J. Klimczak, Jia Yu Koh, Alexander Krasnitz, Nicole Kuderer, Tahsin Kurc, David J. Kwiatkowski, Teresa Laguna, Martin Lang, Anna Lasorella, Thuc D. Le, Adrian V. Lee, Ju-Seog Lee, Steve Lefever, Kjong Lehmann, Jake Leighton, Chunyan Li, Lei Li, Shulin Li, David Liu, Eric Minwei Liu, Jianfang Liu, Rongjie Liu, Yang Liu, William J.R. Longabaugh, Nuria Lopez-Bigas, Li Ma, Wencai Ma, Karen MacKenzie, Andrzej Mackiewicz, Dejan Maglic, Raunaq Malhotra, Tathiane M. Malta, Calena Marchand, R. Jay Mashl, Sylwia Mazurek, Pieter Mestdagh, Chase Miller, Marco Mina, Lopa Mishra, Younes Mokrab, Raymond Monnat, Jr., Nate Moore, Nathanael Moore, Loris Mularoni, Niranjan Nagarajan, Aaron M. Newman, Vu Nguyen, Michael L. Nickerson, Akinyemi I. Ojesina, Catharina Olsen, Sandra Orsulic, Tai-Hsien Ou Yang, James Palacino, Yinghong Pan, Elena Papaleo, Sagar Patil, Chandra Sekhar Pedamallu, Shouyong Peng, Xinxin Peng, Arjun Pennathur, Curtis R. Pickering, Christopher L. Plaisier, Laila Poisson, Eduard Porta-Pardo, Marcos Prunello, John L. Pulice, Charles Rabkin, Janet S. Rader, Kimal Rajapakshe, Aruna Ramachandran, Shuyun Rao, Xiayu Rao, Benjamin J. Raphael, Gunnar Rätsch, Brendan Reardon, Christopher J. Ricketts, Jason Roszik, Carlota Rubio- Perez, Ryan Russell, Anil Rustgi, Russell Ryan, Mohamad Saad, Thais Sabedot, Joel Saltz, Dimitris Samaras, Franz X. Schaub, Barbara G. Schneider, Adam Scott, Michael Seiler, Sara Selitsky, Sohini Sengupta, Jose A. Seoane, Jonathan S. Serody, Reid Shaw, Yang Shen, Tiago Silva, Pankaj Singh, I.K. Ashok Sivakumar, Christof Smith, Artem Sokolov, Junyan Song, Pavel Sumazin, Yutong Sun, Chayaporn Suphavilai, Najeeb Syed, David Tamborero, Alison M. Taylor, Teng Teng, Daniel G. Tiezzi, Collin Tokheim, Nora Toussaint, Mihir Trivedi, Kenneth T. Tsai, Aaron D. Tward, Eliezer Van Allen, John S. Van Arnam, Kristel Van Steen, Carter Van Waes, Christopher P. Vellano, Benjamin Vincent, Nam S. Vo, Vonn Walter, Chen Wang, Fang Wang, Jiayin Wang, Sophia Wang, Wenyi Wang, Yue Wang, Yumeng Wang, Zehua Wang, Zeya Wang, Zixing Wang, Gregory Way, Amila Weerasinghe, Michael Wells, Michael C. Wendl, Cecilia Williams, Joseph Willis, Denise Wolf, Karen Wong, Yonghong Xiao, Lu Xinghua, Bo Yang, Da Yang, Liuqing Yang, Kai Ye, Hiroyuki Yoshida, Lihua Yu, Sobia Zaidi, Huiwen Zhang, Min Zhang, Xiaoyang Zhang, Tianhao Zhao, Wei Zhao, Zhongming Zhao, Tian Zheng, Jane Zhou, Zhicheng Zhou, Hongtu Zhu, Ping Zhu, Michael T. Zimmermann, Elad Ziv, and Patrick A. Zweidler-McKay

The members of The Cancer Genome Atlas Research Network for this project are

NCI/NHGRI Project Team

Samantha J. Caesar-Johnson, John A. Demchok, Ina Felau, Melpomeni Kasapi, Martin L. Ferguson, Carolyn M. Hutter, Heidi J. Sofia, Roy Tarnuzzer, Zhining Wang, Liming Yang, Jean C. Zenklusen, Jiashan (Julia) Zhang

TCGA DCC

Sudha Chudamani, Jia Liu, Laxmi Lolla, Rashi Naresh, Todd Pihl, Qiang Sun, Yunhu Wan, Ye Wu

Genome Data Analysis Centers (GDACs)

The Broad Institute—Juok Cho, Timothy DeFreitas, Scott Frazer, Nils Gehlenborg, Gad Getz, David I. Heiman, Jaegil Kim, Michael S. Lawrence, Pei Lin, Sam Meier, Michael S. Noble, Gordon Saksena, Doug Voet, Hailei Zhang

Institute for Systems Biology—Brady Bernard, Nyasha Chambwe, Varsha Dhankani, Theo Knijnenburg, Roger Kramer, Kalle Leinonen, Yuexin Liu, Michael Miller, Sheila Reynolds, Ilya Shmulevich, Vesteinn Thorsson, Wei Zhang

MD Anderson Cancer Center—Rehan Akbani, Bradley M. Broom, Apurva M. Hegde, Zhenlin Ju, Rupa S. Kanchi, Anil Korkut, Jun Li, Han Liang, Shiyun Ling, Wenbin Liu, Yiling Lu, Gordon B. Mills, Kwok-Shing Ng, Arvind Rao, Michael Ryan, Jing Wang, John N. Weinstein, Jiexin Zhang

Memorial Sloan Kettering Cancer Center—Adam Abeshouse, Joshua Armenia, Debyani Chakravarty, Walid K. Chatila, Ino de Bruijn, Jianjiong Gao, Benjamin E. Gross, Zachary J. Heins, Ritika Kundra, Konnor La, Marc Ladanyi, Augustin Luna, Moriah G. Nissan, Angelica Ochoa, Sarah M. Phillips, Ed Reznik, Francisco Sanchez-Vega, Chris Sander, Nikolaus Schultz, Robert Sheridan, S. Onur Sumer, Yichao Sun, Yichao Sun, Barry S. Taylor, Jioajiao Wang, Hongxin Zhang

Oregon Health and Science University—Pavana Anur, Myron Peto, Paul Spellman

University of California Santa Cruz—Christopher Benz, Joshua M. Stuart, Christopher K. Wong, Christina Yau

University of North Carolina at Chapel Hill—D. Neil Hayes, Joel S. Parker, Matthew D. Wilkerson

Genome Characterization Centers (GCC)

BC Cancer Agency—Adrian Ally, Miruna Balasundaram, Reanne Bowlby, Denise Brooks, Rebecca Carlsen, Eric Chuah, Noreen Dhalla, Robert Holt, Steven J.M. Jones, Katayoon Kasaian, Darlene Lee, Yussanne Ma, Marco A. Marra, Michael Mayo, Richard A.

Moore, Andrew J. Mungall, Karen Mungall, A. Gordon Robertson, Sara Sadeghi, Jacqueline E. Schein, Payal Sipahimalani, Angela Tam, Nina Thiessen, Kane Tse, Tina Wong

The Broad Institute—Ashton C. Berger, Rameen Beroukhim, Andrew D. Cherniack, Carrie Cibulskis, Stacey B. Gabriel, Galen F. Gao, Gavin Ha, Matthew Meyerson, Gordon Saksena, Steven E. Schumacher, Juliann Shih

Harvard—Melanie H. Kucherlapati, Raju S. Kucherlapati

Johns Hopkins—Stephen Baylin, Leslie Cope, Ludmila Danilova

University of Southern California—Moiz S. Bootwalla, Phillip H. Lai, Dennis T. Maglinte, David J. Van Den Berg, Daniel J. Weisenberger

University of North Carolina at Chapel Hill—J. Todd Auman, Saianand Balu, Tom Bodenheimer, Cheng Fan, D. Neil Hayes, Katherine A. Hoadley, Alan P. Hoyle, Stuart R. Jefferys, Corbin D. Jones, Shaowu Meng, Piotr A. Mieczkowski, Lisle E. Mose, Joel S. Parker, Amy H. Perou, Charles M. Perou, Jeffrey Roach, Yan Shi, Janae V. Simons, Tara Skelly, Matthew G. Soloway, Donghui Tan, Umadevi Veluvolu, Matthew D. Wilkerson

Van Andel Research Institute—Huihui Fan, Toshinori Hinoue, Peter W. Laird, Hui Shen, Wanding Zhou

Genome Sequencing Centers (GSC)

Baylor College of Medicine—Michelle Bellair, Kyle Chang, Kyle Covington, Chad J. Creighton, Huyen Dinh, HarshaVardhan Doddapaneni, Lawrence A. Donehower, Jennifer Drummond, Richard A. Gibbs, Robert Glenn, Walker Hale, Yi Han, Jianhong Hu, Viktoriya Korchina, Sandra Lee, Lora Lewis, Wei Li, Xiuping Liu, Margaret Morgan, Donna Morton, Donna Muzny, Jireh Santibanez, Margi Sheth, Eve Shinbrot, Linghua Wang, Min Wang, David A. Wheeler, Liu Xi, Fengmei Zhao

The Broad Institute—Carrie Cibulskis, Stacy B. Gabriel, Julian Hess

Washington University at St. Louis—Elizabeth L. Appelbaum, Matthew Bailey, Matthew G. Cordes, Li Ding, Catrina C. Fronick, Lucinda A. Fulton, Robert S. Fulton, Cyriac Kandoth, Elaine R. Mardis, Michael D. McLellan, Christopher A. Miller, Heather K. Schmidt, Richard K. Wilson

Bio specimen Core Resource

The International Genomics Consortium—Daniel Crain, Erin Curley, Johanna Gardner, Kevin Lau, David Mallery, Scott Morris, Joseph Paulauskis, Robert Penny, Candace Shelton, Troy Shelton, Mark Sherman, Eric Thompson, Peggy Yena

Nationwide Children's Organization—Jay Bowen, Julie M. Gastier-Foster, Mark Gerken, Kristen M. Leraas, Tara M. Lichtenberg, Nilsa C. Ramirez, Lisa Wise, Erik Zmuda

Tissue Source Sites

Australian Prostate Cancer Research Center—Niall Corcoran, Tony Costello, Christopher Hovens

Barretos Cancer Hospital—Andre L. Carvalho, Ana C. de Carvalho, José H. Fregnani, Adhemar Longatto-Filho, Rui M. Reis, Cristovam Scapulatempo-Neto, Henrique C. S. Silveira, Daniel O. Vidal

Barrow Neurological Institute—Andrew Burnette, Jennifer Eschbacher, Beth Hermes, Ardene Noss, Rosy Singh

Baylor College of Medicine—Matthew L. Anderson, Patricia D. Castro, Michael Ittmann

BC Cancer Agency—David Huntsman

BioreclamationIVT—Bernard Kohl, Xuan Le, Richard Thorp

Boston Medical Center—Chris Andry, Elizabeth R. Duffy

Botkin Hospital—Vladimir Lyadov, Oxana Paklina, Galiya Setdikova, Alexey Shabunin, Mikhail Tavobilov

Brain Tumor Center at the University of Cincinnati Gardner Neuroscience Institute—Christopher McPherson, Ronald Warnick

Brigham and Women's Hospital—Ross Berkowitz, Daniel Cramer, Colleen Feltmate, Neil Horowitz, Adam Kibel, Michael Muto, Chandrajit P. Raut

Capital Biosciences, Inc—Andrei Malykh

Case Comprehensive Cancer Center—Jill S. Barnholtz-Sloan, Wendi Barrett, Karen Devine, Jordonna Fulop, Quinn T. Ostrom, Kristen Shimmel, Yingli Wolinsky

Case Western Reserve School of Medicine—Andrew E. Sloan

Catholic University of the Sacred Heart—Agostino De Rose, Felice Giuliante

Cedars-Sinai Medical Center—Marc Goodman, Beth Y. Karlan

Central Arkansas Veterans Healthcare System—Curt H. Hagedorn

Centura Health—John Eckman, Jodi Harr, Jerome Myers, Kelinda Tucker, Leigh Anne Zach

Chan Soon-Shiong Institute of Molecular Medicine at Windber—Brenda Deyarmin, Hai Hu, Leonid Kvecher, Caroline Larson, Richard J. Mural, Stella Somiari

Charles University—Ales Vicha, Tomas Zelinka

Christiana Care Health System—Joseph Bennett, Mary Iacocca, Brenda Rabeno, Patricia Swanson

CHU of Montreal—Mathieu Latour

CHU of Quebec—Louis Lacombe, Bernard Têtu

CHU of Quebec, Laval University Research Center of Chus—Alain Bergeron

Cleveland Clinic Foundation—Mary McGraw, Susan M. Staugaitis

Columbia University—John Chabot, Hanina Hibshoosh, Antonia Sepulveda, Tao Su, Timothy Wang

Cureline, Inc—Olga Potapova, Olga Voronina

Curie Institute—Laurence Desjardins, Odette Mariani, Sergio Roman-Roman, Xavier Sastre, Marc-Henri Stern

Dana-Farber Cancer Institute—Feixiong Cheng, Sabina Signoretti

Dignity Health Mercy Gilbert Medical Center—Jennifer Eschbacher

Duke University Medical Center—Andrew Berchuck, Darell Bigner, Eric Lipp, Jeffrey Marks, Shannon McCall , Roger McLendon, Angeles Secord, Alexis Sharp

Emory University—Madhusmita Behera, Daniel J. Brat, Amy Chen, Keith Delman, Seth Force, Fadlo Khuri, Fadlo Khuri, Kelly Magliocca, Shishir Maithel, Jeffrey J. Olson, Taofeek Owonikoko, Alan Pickens, Suresh Ramalingam, Dong M. Shin, Gabriel Sica, Gabriel Sica, Erwin G. Van Meir, Erwin G. Van Meir, Hongzheng Zhang

Erasmus Medical Center—Wil Eijckenboom, Ad Gillis, Esther Korpershoek, Leendert Looijenga, Wolter Oosterhuis, Hans Stoop, Kim E. van Kessel, Ellen C. Zwarthoff

Foundation of the Carlo Besta Neurological Institute, IRCCS—Chiara Calatozzolo, Lucia Cuppini, Stefania Cuzzubbo, Francesco DiMeco, Gaetano Finocchiaro, Luca Mattei, Alessandro Perin, Bianca Pollo

Fred Hutchinson Cancer Research Center—Chu Chen, John Houck, Pawadee Lohavanichbutr

Friedrich-Alexander-University—Arndt Hartmann, Christine Stoehr, Robert Stoehr, Helge Taubert, Sven Wach, Bernd Wullich

Greater Poland Cancer Center—Witold Kycler, Dawid Murawa, Maciej Wiznerowicz

Greenville Health System Institute for Translational Oncology Research—Ki Chung, W. Jeffrey Edenfield, Julie Martin

Gustave Roussy institute—Eric Baudin

Harvard University—Glenn Bubley, Raphael Bueno, Assunta De Rienzo, William G. Richards

Henry Ford Health System—Ana deCarvalho, Steven Kalkanis, Tom Mikkelsen, Tom Mikkelsen, Houtan Noushmehr, Lisa Scarpace

Hospices Civils de Lyon—Nicolas Girard

Hospital Clinic—Marta Aymerich, Elias Campo, Eva Giné, Armando López Guillermo

Hue Central Hospital—Nguyen Van Bang, Phan Thi Hanh, Bui Duc Phu

Human Tissue Resource Network—Yufang Tang

Huntsman Cancer Institute—Howard Colman, Kimberley Evason

Icahn School of Medicine at Mount Sinai—Peter R. Dottino, John A. Martignetti

Imperial College London—Hani Gabra

Indivumed GmbH—Hartmut Juhl

Institute of Human Virology Nigeria—Teniola Akeredolu

Institute of Urgent Medicine—Serghei Stepa

John Wayne Cancer Institute—Dave Hoon

Keimyung University—Keunsoo Ahn, Koo Jeong Kang

Ludwich Maximilians University Munich—Felix Beuschlein

Maine Medical Center—Anne Breggia

Massachusetts General Hospital—Michael Birrer

Mayo Clinic—Debra Bell, Mitesh Borad, Alan H. Bryce, Erik Castle, Vishal Chandan, John Cheville, John A. Copland, Michael Farnell, Thomas Flotte, Nasra Giama, Thai Ho, Michael Kendrick, Jean-Pierre Kocher, Karla Kopp, Catherine Moser, David Nagorney, Daniel O'Brien, Brian Patrick O'Neill, Tushar Patel, Gloria Petersen, Gloria Petersen, Florencia Que, Michael Rivera, Lewis Roberts, Robert Smallridge, Robert Smallridge,

Thomas Smyrk, Thomas Smyrk, Melissa Stanton, R. Houston Thompson, Michael Torbenson, Ju Dong Yang, Lizhi Zhang, Lizhi Zhang

McGill University Health Center—Fadi Brimo

MD Anderson Cancer Center—Jaffer A. Ajani, Ana Maria Angulo Gonzalez, Carmen Behrens, Jolanta Bondaruk, Russell Broaddus, Bradley Broom, Bogdan Czerniak, Bita Esmaeli, Junya Fujimoto, Jeffrey Gershenwald, Charles Guo, Alexander J. Lazar, Christopher Logothetis, Funda Meric-Bernstam, Funda Meric-Bernstam, Cesar Moran, Lois Ramondetta, David Rice, Anil Sood, Pheroze Tamboli, Timothy Thompson, Patricia Troncoso, Patricia Troncoso, Anne Tsao, Ignacio Wistuba

Melanoma Institute Australia—Candace Carter, Lauren Haydu, Peter Hersey, Valerie Jakrot, Hojabr Kakavand, Richard Kefford, Kenneth Lee, Georgina Long, Graham Mann, Michael Quinn, Robyn Saw, Richard Scolyer, Kerwin Shannon, Andrew Spillane, Jonathan Stretch, Maria Synott, John Thompson, James Wilmott

Memorial Sloan Kettering Cancer Center—Hikmat Al-Ahmadie, Timothy A. Chan, Ronald Ghossein, Anuradha Gopalan, Douglas A. Levine, Victor Reuter, Samuel Singer, Bhuvanesh Singh

Ministry of Health of Vietnam—Nguyen Viet Tien

Molecular Response—Thomas Broudy, Cyrus Mirsaidi, Praveen Nair

Nancy N. and J.C. Lewis Cancer & Research Pavilion at St. Joseph's/Candler —Paul Drwiega, Judy Miller, Jennifer Smith, Howard Zaren

National Cancer Center Korea—Joong-Won Park

National Cancer Hospital of Vietnam—Nguyen Phi Hung

National Cancer Institute—Electron Kebebew, W. Marston Linehan, Adam R. Metwalli, Karel Pacak, Peter A. Pinto, Mark Schiffman, Laura S. Schmidt, Cathy D. Vocke, Nicolas Wentzensen, Robert Worrell, Hannah Yang

Norfolk & Norwich University Hospital—Marc Moncrieff

NYU Langone Medical Center—Chandra Goparaju, Jonathan Melamed, Harvey Pass

Oncology Institute—Natalia Botnariuc, Irina Caraman, Mircea Cernat, Inga Chemencedji, Adrian Clipca, Serghei Doruc, Ghenadie Gorincioi, Sergiu Mura, Maria Pirtac, Irina Stancul, Diana Tcaciuc

Ontario Tumour Bank—Monique Albert, Iakovina Alexopoulou, Angel Arnaout, John Bartlett, Jay Engel, Sebastien Gilbert, Jeremy Parfitt, Harman Sekhon

Oregon Health & Science University—George Thomas

Papworth Hospital NHS Foundation Trust—Doris M. Rassl, Robert C. Rintoul

Providence Health and Services—Carlo Bifulco, Raina Tamakawa, Walter Urba

QIMR Berghofer Medical Research Institute—Nicholas Hayward

Radboud Medical University Center—Henri Timmers

Regina Elena National Cancer Institute—Anna Antenucci, Francesco Facciolo, Gianluca Grazi, Mirella Marino, Roberta Merola

Reinier de Graaf Hospital—Ronald de Krijger

René Descartes University—Anne-Paule Gimenez-Roqueplo

Research Center of Chus Sherbrooke, Québec—Alain Piché

Research Institute of the McGill University Health Centre—Simone Chevalier, Ginette McKercher

Rockefeller University—Kivanc Birsoy

Rose Ella Burkhardt Brain Tumor and Neuro-Oncology Center—Gene Barnett, Cathy Brewer, Carol Farver, Theresa Naska, Nathan A. Pennell, Daniel Raymond, Cathy Schilero, Kathy Smolenski, Felicia Williams

Roswell Park Cancer Institute—Carl Morrison

Rush University—Jeffrey A. Borgia, Michael J. Liptay, Mark Pool, Christopher W. Seder

Saarland University—Kerstin Junker

Sage Bionetworks—Larsson Omberg

Saint-Petersburg City Clinical Oncology Hospital—Mikhail Dinkin, George Manikhas

Sapienza University of Rome—Domenico Alvaro, Maria Consiglia Bragazzi, Vincenzo Cardinale, Guido Carpino, Eugenio Gaudio

Spectrum Health—David Chesla, Sandra Cottingham

St. Petersburg Academic University RAS—Michael Dubina, Fedor Moiseenko

Stanford University—Renumathy Dhanasekaran

Technical University of Munich—Karl-Friedrich Becker, Klaus-Peter Janssen, Julia Slotta-Huspenina

The International Genomics Consortium—Daniel Crain, Erin Curley, Johanna Gardner, David Mallery, Scott Morris, Joseph Paulauskis, Robert Penny, Candace Shelton, Troy Shelton, Eric Thompson

The Ohio State University—Mohamed H. Abdel-Rahman, Dina Aziz, Sue Bell, Colleen M. Cebulla, Amy Davis, Rebecca Duell, J. Bradley Elder, Joe Hilty, Bahavna Kumar, James Lang, Norman L. Lehman, Randy Mandt, Phuong Nguyen, Robert Pilarski, Karan Rai, Lynn Schoenfield, Kelly Senecal, Paul Wakely

The Oregon Clinic—Paul Hansen

The Research Institute at Nationwide Children's Hospital—Nilsa Ramirez

Tufts Medical Center—Ronald Lechan, James Powers, Arthur Tischler

University of Alabama at Birmingham Medical Center—William E. Grizzle, Katherine C. Sexton

UC Cancer Institute—Alison Kastl

UCSF-Helen Diller Family Comprehensive Cancer Center—Joel Henderson, Sima Porten

University Hospital of Giessen and Marburg—Jens Waldmann

University Hospital in Wurzburg, Germany—Martin Fassnacht

University Health Network—Sylvia L. Asa

University Hospital Essen—Dirk Schadendorf

University Hospitals Case Medical Center Hamburg-Eppendorf—Marta Couce, Markus Graefen, Hartwig Huland, Guido Sauter, Thorsten Schlomm, Ronald Simon, Pierre Tennstedt

University of Abuja Teaching Hospital—Oluwole Olabode

University of Arizona—Mark Nelson

University of Calgary—Oliver Bathe

University of California—Peter R. Carroll, June M. Chan, Philip Disaia, Pat Glenn, Robin K. Kelley, Charles N. Landen, Joanna Phillips, Michael Prados, Jeff Simko, Jeffry Simko, Karen Smith-McCune, Scott VandenBerg

University of Chicago Medicine—Kevin Roggin

University of Cincinnati—Ashley Fehrenbach, Ady Kendler

University of Cincinnati Cancer Institute—Suzanne Sifri, Ruth Steele

University of Colorado Cancer Center—Antonio Jimeno

University of Dundee—Francis Carey, Ian Forgie

University of Florence—Massimo Mannelli

University of Hawaii Cancer Center—Michael Carney, Brenda Hernandez

University of Heidelberg—Benito Campos, Christel Herold-Mende, Christin Jungk, Andreas Unterberg, Andreas von Deimling

University of Iowa Hospital & Clinics—Aaron Bossler, Joseph Galbraith, Laura Jacobus, Michael Knudson, Tina Knutson, Deqin Ma, Mohammed Milhem, Rita Sigmund

University of Kansas Medical Center—Andrew K. Godwin, Rashna Madan, Howard G. Rosenthal

University of Maryland School of Medicine—Clement Adebamowo, Sally N. Adebamowo

University of Melbourne—Alex Boussioutas

University of Michigan—David Beer, Thomas Giordano

University of Montreal—Anne-Marie Mes-Masson, Fred Saad

University of New Mexico—Therese Bocklage

University of Oklahoma—Lisa Landrum, Robert Mannel, Kathleen Moore, Katherine Moxley, Russel Postier, Joan Walker, Rosemary Zuna

University of Pennsylvania—Michael Feldman, Federico Valdivieso

University of Pittsburgh—Rajiv Dhir, James Luketich

University of Puerto Rico—Edna M. Mora Pinero, Mario Quintero-Aguilo

University of São Paulo—Carlos Gilberto Carlotti Junior, Jose Sebastião Dos Santos, Rafael Kemp, Ajith Sankarankuty, Daniela Tirapelli

University of Sheffield Western Bank—James Catto

University of Washington—Kathy Agnew, Elizabeth Swisher

University of Western Australia—Jenette Creaney, Bruce Robinson

University of Wisconsin School of Medicine and Public Health—Carl Simon Shelley

University of Kansas Cancer Center—Eryn M. Godwin, Sara Kendall, Cassaundra Shipman

University of Michigan—Carol Bradford, Thomas Carey, Andrea Haddad, Jeffey Moyer, Lisa Peterson, Mark Prince, Laura Rozek, Gregory Wolf

UQ Thoracic Research Centre—Rayleen Bowman, Kwun M. Fong, Ian Yang

Valley Health System—Robert Korst

Vanderbilt University Medical Center—W. Kimryn Rathmell

Walter Reed National Medical Center—J. Leigh Fantacone-Campbell, Jeffrey A. Hooke, Albert J. Kovatich, Craig D. Shriver

Washington University—John DiPersio, Bettina Drake, Ramaswamy Govindan, Sharon Heath, Timothy Ley, Brian Van Tine, Peter Westervelt

Weill Cornell Medical College—Mark A. Rubin

Yonsei University College of Medicine—Jung Il Lee

Institution Not Provided—Natália D. Aredes, Armaz Mariamidze

TCGA Pan-LncRNA AWG

University of Pittsburgh—Yue Wang

Institution Addresses

Australian Prostate Cancer Research Center, Epworth Hospital, VIC, Australia

Australian Prostate Cancer Research Center, Epworth Hospital, VIC, Australia

Barretos Cancer Hospital, Av: Antenor Duarte Villela, 1331, Barretos, São Paulo, Brazil

Barrow Neurological Institute, St. Joseph's Hospital and Medical Center, Phoenix, Arizona 85013

Barrow Neurological Institute, St. Joseph's Hospital and Medical Center, Phoenix, Arizona 85013,

Baylor College of Medicine One Baylor Plaza, Houston, TX 77030

BC Cancer Agency, 675 W 10th Ave, Vancouver, BC V5Z 1L3, Canada

Beth Israel Deaconess Medical Center Harvard University Medical School Boston Mass

BioreclamationIVT, 99 Talbot Blvd Chestertown, MD 21620

Boston Medical Center, Boston MA 02118

Botkin Hospital, 2-y Botkinskiy pr-d, 5, Moskva, Russia, 125284

Brain Tumor and Neuro-oncology Center, Department of Neurosurgery, University Hospitals Case Medical Center, Case Western Reserve School of Medicine, 11100 Euclid Ave, Cleveland, Ohio, 44106

Brain Tumor Center at the University of Cincinnati Gardner Neuroscience Institute, and Department of Neurosurgery, University of Cincinnati College of Medicine, and Mayfield Clinic, 260 Stetson Street, Suite 2200, Cincinnati, Ohio, 45219

Brain Tumor Center at the University of Cincinnati Neuroscience Institute, and Department of Neurosurgery, University of Cincinnati College of Medicine, and Mayfield Clinic, 234 Goodman Street, Cincinnati, Ohio, 45219

Brigham and Women's Hospital, 75 Francis St, Boston MA 02115

Capital Biosciences, Inc., 900 Clopper Rd, Suite 120, Gaithersburg, MD 20878

Case Comprehensive Cancer Center, 11100 Euclid Ave - Wearn 152, Cleveland, OH 44106-5065

Cedars-Sinai Medical Center, 8700 Beverly Boulevard, Suite 290 West MOT, Los Angeles, CA

Center for Liver Cancer, National Cancer Center Korea, 323 Ilsan-ro, Ilsan dong-gu, Goyang, Gyeonggi 10408, South Korea

Central Arkansas Veterans Healthcare System, Little Rock, AR 72205

CHU of Quebec, Laval University Research Center of Chus 2705, boul. Laurier Bureau TR72 QUÉBEC, Quebec G1V 4G2

Centura Health 9100 E Mineral Cir, Centennial, CO 80112

Chan Soon-Shiong Institute of Molecular Medicine at Windber, Windber, PA 15963

Charles University, Czech Republic

CHU of Quebec, Hôtel-Dieu de Quebec-University Laval, 11 cote du palais, Quebec City, G1R 2J6

CHUM, Montreal, Qc, Canada.

Clinic of Urology and Pediatric Urology, Saarland University, Homburg, Germany.

Clinical Breast Care Project, Murtha Cancer Center, Uniformed Services University / Walter Reed National Military Medical Center, Bethesda, MD 20889

Comprehensive Cancer Center Tissue Procurement Shared Resource, Cooperative Human Tissue Network Midwestern Division, Dept. of Pathology, Human Tissue Resource Network, The Ohio State University, 410 West 10th Ave, Doan Hall, Room E413A, Columbus, OH 43210

Cureline, Inc., 290 Utah Ave, Ste 300, South san Francisco, CA 94080, USA

Dana-Farber Cancer Institute, 450 Brookline Ave, Boston MA, 02215

Dardinger Neuro-Oncology Center, Department of Neurosurgery, James Comprehensive Cancer Center and The Ohio State University Medical Center, 320 W 10th Ave, Columbus, Ohio, 43210

Department of Cardiovascular and Thoracic Surgery. Suite 774 Professional Office Building. 1735 W. Harrison St., Chicago, IL 60612

Department of Epidemiology and Public Health, University of Maryland School of Medicine, Baltimore MD 21201

Department of Genetics & Genomic Sciences, Icahn School of Medicine at Mount Sinai, 1 Gustave L. Levy Place, New York, NY 10029

Department of Hematology and Medical Oncology, Mayo Clinic Arizona, 5779 E. Mayo Blvd, Phoenix AZ 85054

Department of Medicine, University of Wisconsin School of Medicine and Public Health, 1685 Highland Avenue, Madison, WI 53705

Department of Medicine, Washington University in St. Louis, 660 S. Euclid Ave., CB 8066, St. Louis, MO 63110

Department of Medicine, Yonsei University College of Medicine, Seoul, Republic of Korea

Department of Neurological Surgery

Department of Neurosurgery, Emory University School of Medicine, 1365 Clifton Road, NE, Atlanta, GA 30322

Department of Obstetrics and Gynecology, Baylor College of Medicine, One Baylor Plaza, Houston, Texas 77030

Department of Obstetrics/Gynecology and Reproductive Sciences, Icahn School of Medicine at Mount Sinai, 1 Gustave L. Levy Place, New York, NY 10029

Department of Orthopedic Surgery, University of Kansas Medical Center 3901 Rainbow Boulevard, Kansas City, KS 66160

Department of Pathology and Cell Biology, Columbia University, New York, NY10032

Department of Pathology and Immunology, Baylor College of Medicine, One Baylor Plaza, Houston, TX 77030

Department of Pathology and Laboratory Medicine, University of Kansas Medical Center, Kansas City, KS 66206

Department of Pathology, Department of Cell and Molecular Medicine. 570 Jelke South center, 1750 W. Harrison St., Chicago, IL 60612

Department of Pathology, Duke University School of Medicine, Durham, NC 27710

Department of Pathology, Spectrum Health, 35 Michigan NE, Grand Rapids, MI 49503

Department of Pathology, The Ohio State University School of Medicine, N308 Doan Hall, 410 W 10th Ave, Columbus, OH-43210-1267

Department of Pathology, The Ohio State University Wexner Medical Center (Doan Hall N337B, 410 West 10th Ave., Columbus, OH 43210)

Department of Pathology. 570 Jelke South center, 1750 W. Harrison St., Chicago, IL 60612

Department of Surgery and Anatomy, Ribeirão Preto Medical School - FMRP, University of São Paulo, Brazil, 14049-900

Department of Surgery and Cancer, Imperial College London, Du Cane Road London W12 0NN, UK

Department of Surgery, Brigham and Women's Hospital, Harvard Medical School, Boston, MA, USA

Department of Surgery, Columbia University, New York, NY 10032

Department of Surgery, University of Michigan, Ann Arbor MI 48109

Department of Urology and Pediatric Urology, University Hospital Erlangen, Friedrich-Alexander-University Erlangen-Nuremberg, 91054 Erlangen, Germany

Department of Urology, Mayo Clinic Arizona, 5779 E. Mayo Blvd, Phoenix AZ 85054

Departments of Neurosurgery and Hematology and Medical Oncology, School of Medicine and Winship Cancer Institute, 1365C Clifton Rd. N.E., Emory University, Atlanta, GA 30322

Departments of Pathology & Translational Molecular Pathology, The University of Texas MD Anderson Cancer Center, 1515 Holcombe Blvd--Unit 85, Houston, Texas, USA

Dept. of Pathology & Laboratory Medicine, University of Cincinnati, UC Health University Hospital, 234 Goodman Street, Cincinnati, OH 45219-0533

Dept. of Pathology, Robert J. Tomsich Pathology & Laboratory Medicine Institute, Lerner Research Inst, Cleveland Clinic Foundation, Cleveland, OH 44195

Dept. of Surgery, Klinikum rechts der Isar, Technical University of Munich, Ismaninger Str. 22, 81675 Munich, Germany

Dignity Health Mercy Gilbert Medical Center 3555 S Val Vista Dr, Gilbert, AZ 85297

Division Molecular Urology, Department of Urology and Pediatric Urology, University Hospital Erlangen, Friedrich-Alexander-University Erlangen-Nuremberg, 91054 Erlangen, Germany

Division of Cancer Epidemiology and Genetics, National Cancer Institute, 9609 Medical Center Dr. Bethesda 20892 USA

Division of Neurosurgical Research, Dpt. Neurosurgery, University of Heidelberg, INF 400, 69120 Heidelberg, Germany

Division of Surgical Oncology, Department of Surgery, Brigham and Women's Hospital, 75 Francis Street, Boston, MA 02115

Dpt. Neuropathology, University of Heidelberg, INF 224, 69120 Heidelberg, Germany

Dpt. Neurosurgery, University of Heidelberg, INF 400, 69120 Heidelberg, Germany

Duke University

Duke University Medical Center 177 MSRB Box 3156 Durham, NC 27710

Duke University Medical Center, Gynecologic Oncology, Box 3079, Durham, NC USA

Emory University, 1365 Clifton Road, NE Atlanta GA, 30322

Erasmus MC, Wytemaweg 80, 3015 CN, Rotterdam, The Netherlands

Erasmus Medical Center

Erasmus University Medical Center Rotterdam, Cancer Institute, Wytemaweg 80, 3015CN, Rotterdam, the Netherlands

The Foundation of the Carlo Besta Neurological Institute, IRCCS via Celoria 11, 20133

Fred Hutchinson Cancer Research Center, 1100 Fairview Ave N, Seattle, WA 98019

Greater Poland Cancer Center, Garbary 15, 61-866 Poznań Poland

Greenville Health System Institute for Translational Oncology Research 900 West Faris Road Greenville SC 29605

Harvard University Cambridge, MA 02138

Havener Eye Institute, The Ohio State University Wexner Medical Center 915 Olentangy River Rd, Columbus, OH 43212

Henry Ford Hospital 2799 West Grand Blvd Detroit MI USA 48202

Hepatobiliary Surgery Unit, A. Gemelli Hospital, Catholic University of the Sacred Heart, Largo Agostino Gemelli 8, 00168 Rome, Italy

Hermelin Brain Tumor Center, Henry Ford Health System, 2799 W Grand Blvd, Detroit, MI, 48202

Hospices Civils de Lyon, CARDIOBIOTEC, Lyon F-69677, France

Hospital Clinic, Villarroel 180, Barcelona, Spain, 08036

Hue Central Hospital, Hue, Vietnam

Human Tissue Resource Network, Dept. of Pathology, College of Medicine, 1615 Polaris Innovation Ctr, 2001 Polaris, Columbus 43240

Huntsman Cancer Institute, Univ. of Utah, 2000 Circle of Hope, Salt Lake City, UT 84112

Indivumed GmbH, 20251 Hamburg, Germany

René Descartes University, Hospital Européen Georges Pompidou, 20 rue Leblanc, 75015, Paris, France

Curie Institute, 26 rue Ulm, 75005 Paris, France

Gustave Roussy Institute of Oncology, 39 Rue Camille Desmoulins 94805, Villejuif, France

Institute of Human Virology Nigeria, Abuja, Nigeria

Institute of Pathology, Technical University of Munich, Trogerstr. 18, 83675 Munich, Germany

Institute of Pathology, University Hospital Erlangen, Firedrich-Alexander-University Erlangen-Nuremberg, 91054 Erlangen, Germany

Institute of Urgent Medicine, Republic of Moldova

Regina Elena National Cancer Institute Irccs - Ifo, Via Elio Chianesi 53, 00144, Rome, Italy

John Wayne Cancer Institute, 2200 Santa Monica Blvd, Santa Monica, CA 90404

Keimyung University, Daegu, South Korea

Knight Comprehensive Cancer Institute, Oregon Health & Science University

Ludwich Maximilians University Munich, Ziemssenstrasse 1, D-80336, Munich, Germany

Maine Medical Center, 22 Bramhall St., Portland, ME 04102

Martini-Clinic, Prostate Cancer Center, University Medical Center Hamburg-Eppendorf, Martinistr. 52, D-20246 Hamburg, Germany

Massachusetts General Hospital 55 Fruit Street Boston Ma 02114

Mayo Clinic 5777 E Mayo Blvd, Phoenix, Arizona 85054

Mayo Clinic 4500 San Pablo Road Jacksonville, FL 32224

Mayo Clinic, 200 First St. SW, Rochester, MN 55905

Mayo Clinic, Rochester, MN 55905

McGill University Health Center. 1001 Decarie Blvd, Montreal, QC, Canada H4A 3J1

MD Anderson Cancer Center 1515 Holcombe Blvd. Unit 0085 Houston, TX 77030

MD Anderson Cancer Center, Department of Pathology, Unit 085; 1515

MD Anderson Cancer Center Life Science Plaza Building 2130 W. Holcombe Blvd, Unit 2951 Houston, TX 77030 Office: LSP9.4029

Melanoma Institute Australia, North Sydney, NSW, Australia 2060

Memorial Sloan Kettering Cancer Center Department of Pathology, 1275 York Avenue, New York, NY 10065

Memorial Sloan Kettering Cancer Center, 1275 York Avenue, New York, NY 10065

Memorial Sloan Kettering Cancer Center, Center for Molecular Oncology, 1275 York Avenue, New York, NY 10065

Ministry of Health of Vietnam, Hanoi, Vietnam

Molecular Pathology Shared Resource of Herbert Irving Comprehensive Cancer Center of Columbia University, New York, NY10032

Molecular Response 11011 Torreyana Road San Diego, CA 92121

Murtha Cancer Center, Uniformed Services University / Walter Reed National Military Medical Center, Bethesda, MD 20889

Nancy N. and J.C. Lewis Cancer & Research Pavilion at St. Joseph's/Candler, 225 Candler Drive, Savannah, GA 31405

National Cancer Hospital of Vietnam

National Cancer Institute, 31 Center Dr, Bethesda, MD 20892

National Cancer Institute, Bethesda, MD 20892

Norfolk & Norwich University Hospital, Norwich, UK. NR4 7UY

NYU Langone Medical Center, Cardiothoracic Surgery, 530 first Avenue, 9V, New York, NY

Oncology Institute, Republic of Moldova

Ontario Tumor Bank - Hamilton site, St. Joseph's Healthcare Hamilton, Hamilton, Ontario L8N 3Z5, Canada

Ontario Tumor Bank - Kingston site, Kingston General Hospital, Kingston, Ontario K7L 5H6, Canada

Ontario Tumor Bank – Ottawa site, The Ottawa Hospital, Ottawa, Ontario K1H 8L6, Canada.

Ontario Tumor Bank, London Health Sciences Centre, London, Ontario N6A 5A5, Canada

Ontario Tumor Bank, Ontario Institute for Cancer Research, Toronto, Ontario M5G 0A3, Canada

Orbital Oncology & Ophthalmic Plastic Surgery Department of Plastic Surgery M.D. Anderson Cancer Center 1515 Holcombe Blvd, Unit 1488 Houston, Texas 77030

Papworth Hospital NHS Foundation Trust, UK

Pathology, St. Joseph's/Candler, 5353 Reynolds St., Savannah, GA 31405

Professor, Division of Neuropathology, Department of Pathology, University Hospitals Case Medical Center

Program in Epidemiology, Fred Hutchinson Cancer Research Center, Seattle, WA 98109

Providence Health and Services

QIMR Berghofer Medical Research Institute, Herston, QLD, Australia

Radboud Medical University Center, Geert Grooteplein-Zuid 10, Nijmegen, the Netherlands

Regina Elena National Cancer Institute, 00144 Rome, Italy

Reinier de Graaf Hospital, Reinier de Graafweg 5, 2625AD, Delft, the Netherlands

Research Institute of the McGill University Health Centre, McGill University, Montréal, Québec, Canada

Research Center Of Chus Sherbrooke, Québec aile 9, porte 6, 3001 12e Avenue Nord, Sherbrooke, QC J1H 5N4, Canada

Rockefeller University 1230 York Ave New York, NY

Rose Ella Burkhardt Brain Tumor and Neuro-Oncology Center ND4-52A, Cleveland Clinic Foundation, 9500 Euclid

Ave, Cleveland, OH 44195

Rose Ella Burkhardt Brain Tumor and Neuro-Oncology Center, 9500 Euclid Avenue - CA51, Cleveland, OH 44195

Rose Ella Burkhardt Brain Tumor and Neuro-Oncology Center, Department of Neurosurgery, Neurological and

Taussig Cancer Institute, Cleveland Clinic, 9500 Euclid Avenue, Cleveland, Ohio, 44195

Roswell Park Cancer Institute. Elm & Carlton Streets, Buffalo NY 14263

Sage Bionetworks, Seattle, WA 98109

Saint-Petersburg City Clinical Oncology Hospital, 56 Veteranov prospect, Saint-Petersburg, 198255, Russia

Sapienza University of Rome, Piazzale Aldo Moro 5, 00185 Rome, Italy

School of Medicine, National Center for Asbestos Related Research, University of Western Australia, Nedlands, WA, Australia 6009

Sir Peter MacCallum Department of Oncology, University of Melbourne, Parkville, 3050, Victoria, Australia

St. Petersburg Academic University RAS, 8/3 Khlopin Str., St. Petersburg, 194021, Russia

Stanford University, Palo Alto, CA, USA

Stephenson Cancer Center, University of Oklahoma, Oklahoma City, OK USA

Tayside Tissue Bank, University of Dundee, Scotland UK DD1 9SY

The International Genomics Consortium, 445 N. 5th Street, Phoenix, Arizona 85004

The Ohio State University, Columbus, OH 43210

The Ohio State University Comprehensive Cancer Center, 320 W 10th Avenue, Columbus, OH 43210

The Ohio State University Wexner Medical Center (2012 Kenny Rd, Columbus, OH 43221)

The Oregon Clinic 1111 NE 99th Ave, Portland, OR 97220

The Prince Charles Hospital, UQ Thoracic Research Centre, Australia 4032

The Research Institute at Nationwide Children's Hospital 700 Children's Drive Columbus Ohio 43205

Tufts Medical center, 800 Washington St. Boston MA 02111

UABMC 401 Beacon Pkwy W Birmingham AL 35209

UC Cancer Institute, 200 Albert Sabin Way, Suite 1012, Cincinnati, OH 45267-0502

UCSF-Helen Diller Family Comprehensive Cancer Center, 550 16th St., Mission Hall WS 6532 Box 3211, San

Francisco, CA 94143

University Hospital of Giessen and Marburg, Badingerstrasse 3, 35044, Marburg, Germany

University Hospital in Wurzburg, Germany, Oberdürrbacher Strasse 6, 97080, Würzburg, Germany

University Health Network, 200 Elizabeth Street, Toronto ON M5G 2C4 Canada

University Hospital Essen, University Duisburg-Essen, German Cancer Consortium, Hufelandstr. 55; 45239 Essen, Germany

University Medical Center Hamburg-Eppendorf, Martinistr. 52, D-20246 Hamburg, Germany

University of Abuja Teaching Hospital, Gwagalada, FCT, Nigeria

University of Arizona Tucson Arizona

University of Calgary, Departments of Surgery and Oncology, 1331 - 29th St NW, Calgary, AB, T2N 4N2

University of California San Francisco, 2340 Sutter St Rm S 229, San Francisco CA 94143

University of California, Irvine 333 City Boulevard West Suite 1400 Orange CA 92868

University of Chicago Medicine 5841 S. Maryland Ave. Room G-216, MC 5094|Chicago, IL 60637

University of Cincinnati Cancer Institute, Brain Tumor Clinical Trials, 200 Albert Sabin Way Suite 1012, Cincinnati,

OH 45267

University of Cincinnati Cancer Institute, Holmes Bldg., 200 Albert Sabin Way, Ste 1002, Cincinnati, OH 45267-0502

University of Colorado Cancer Center, Aurora, CO, 80111, USA

University of Dundee, Scotland UK DD1 9SY

University of Florence, Viale Pieraccini 6, 50139 Firenze, Italy

University of Hawaii Cancer Center

University of Iowa Hospital & Clinics, 200 Hawkins Drive, Clinical Trials-Data Management, 11510 PFP, Iowa City, IA 52242

University of Iowa Hospital & Clinics, 200 Hawkins Drive, Hematology/Oncology, C32 GH, Iowa City, IA 52242

University of Iowa Hospital & Clinics, 200 Hawkins Drive, ICTS-Informatics, 272 MRF, Iowa City, IA 52242

University of Iowa Hospital & Clinics, 200 Hawkins Drive, Medicine Administration, 380 MRC, Iowa City, IA 52242

University of Iowa Hospital & Clinics, 200 Hawkins Drive, Molecular Pathology, B606 GH, Iowa City, IA 52242

University of Iowa Hospital & Clinics, 200 Hawkins Drive, Pathology, SW247 GH, Iowa City, IA 52242

University of Kansas Cancer Center, 3901 Rainbow Blvd, Kansas City, KS. 66160

University of Kansas Medical Center Kansas City KS 66160

University of Michigan 500 S State St, Ann Arbor, MI 48109

University of Montreal 2900 Edouard Mont petit Blvd, Montreal, QC H3T 1J4, Canada

University of New Mexico Albuquerque, New Mexico 87131

University of Pennsylvania Philadelphia, PA 19104

University of Pittsburgh, Department of Cardiothoracic Surgery,200 Lothrop St, Suite C-800, Pittsburgh, Pennsylvania 15213

University of Pittsburgh, Department of Pathology, Pittsburgh, Pennsylvania 15213

University of Sheffield Western Bank, Sheffield S10 2TN, UK

University of Washington Seattle, WA 98105

UPR Comprehensive Cancer Center Biobank; University of Puerto Rico Comprehensive Cancer Center, Celso Barbosa St. Medical Center Area, San Juan, PR 00936

Urologic Oncology Branch, Center for Cancer Research, National Cancer Institute, Building 10, Room 1-5940,

Bethesda, MD 20892-1107

Valley Health System, 1 Valley Health Plaza, Paramus, NJ 07652

Vanderbilt University Medical Center 1211 Medical Center Dr, Nashville, TN 37232

Washington University School of Medicine, 600 S. Taylor Ave, St. Louis, MO 63110

Weill Cornell Medical College, New York, NY 10065

Significance

Although global epigenetic alterations have been established as a prominent cancer hallmark, the epigenetic abnormality of lncRNA loci and their consequences in cancer development remain poorly characterized. We report an in-depth characterization of epigenetic landscape of lncRNA genes in 20 cancer types and discover that the expression of lncRNAs is recurrently epigenetically activated in tumors by hypomethylation. This study provides an integrative strategy of identifying lncRNA genes with oncogenic activity. Using this strategy, we have validated *EPIC1* as an oncogenic lncRNA by interacting with the MYC protein and promoting cell cycle progression. These discoveries expand upon the known mechanisms of MYC activation in cancer and pave the way to develop therapies that target MYC through its interaction with *EPIC1*.

Highlights

- LncRNAs show a hypomethylation phenotype, in contrast to a CIMP phenotype in cancer
- *EPIC1* promotes breast tumorigenesis through regulating cancer cell cycle progression
- *EPIC1* directly interacts with MYC protein through *EPIC1*'s 129–283 nt region
- *EPIC1* regulates MYC targets by enhancing MYC occupancy on its target promoters

Wang et al. characterize the epigenetic landscape of lncRNAs genes across a large number of human tumors and cancer cell lines and observe recurrent hypomethylation of lncRNA genes, including *EPIC1. EPIC1* RNA promotes cell cycle progression by interacting with MYC and enhancing its binding to target genes.

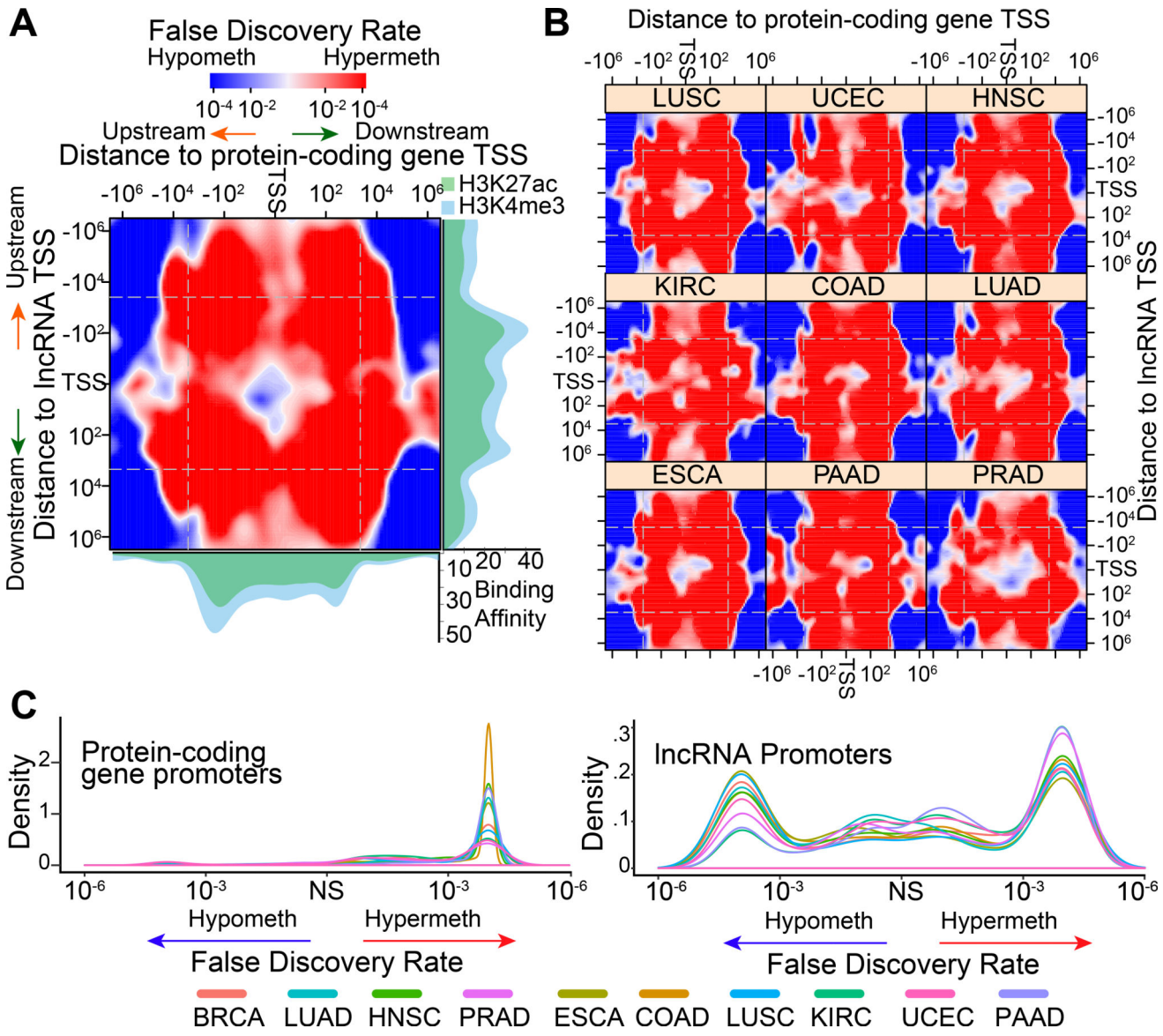

Figure 1. LncRNA and protein coding genes have distinct DNA methylation patterns in ten cancer types

(A) Weighted density plot (kde2d.weighted [package: ggtern]) of differential DNA methylation (indicated by FDR values) of 100 windows within ± 1000 kb from TSS sites are shown in breast cancer tissues. The windows are arranged based on their distances to protein coding gene (PCG) TSS (x-axis) and lncRNA gene TSS (y-axis). The promoter region is defined as ± 3 kb (white dashed lines) from TSS. The hypermethylation region in tumor is shown as red, whereas the hypomethylation region is shown as blue. The average H3K27ac and H3K4me3 binding intensities are shown along with the x and y axes.

(B) Differential DNA methylation between tumors and matched normal tissues in nine cancer types.

(C) Distribution of the differential DNA methylation weighted density values (kde2d.weighted [package: ggtern]) within ± 3 kb region (white dashed lines) of PCG TSS

(left) and lncRNA TSS (right) in ten cancer types. NS, not significant. See also Figure S1 and Table S1.

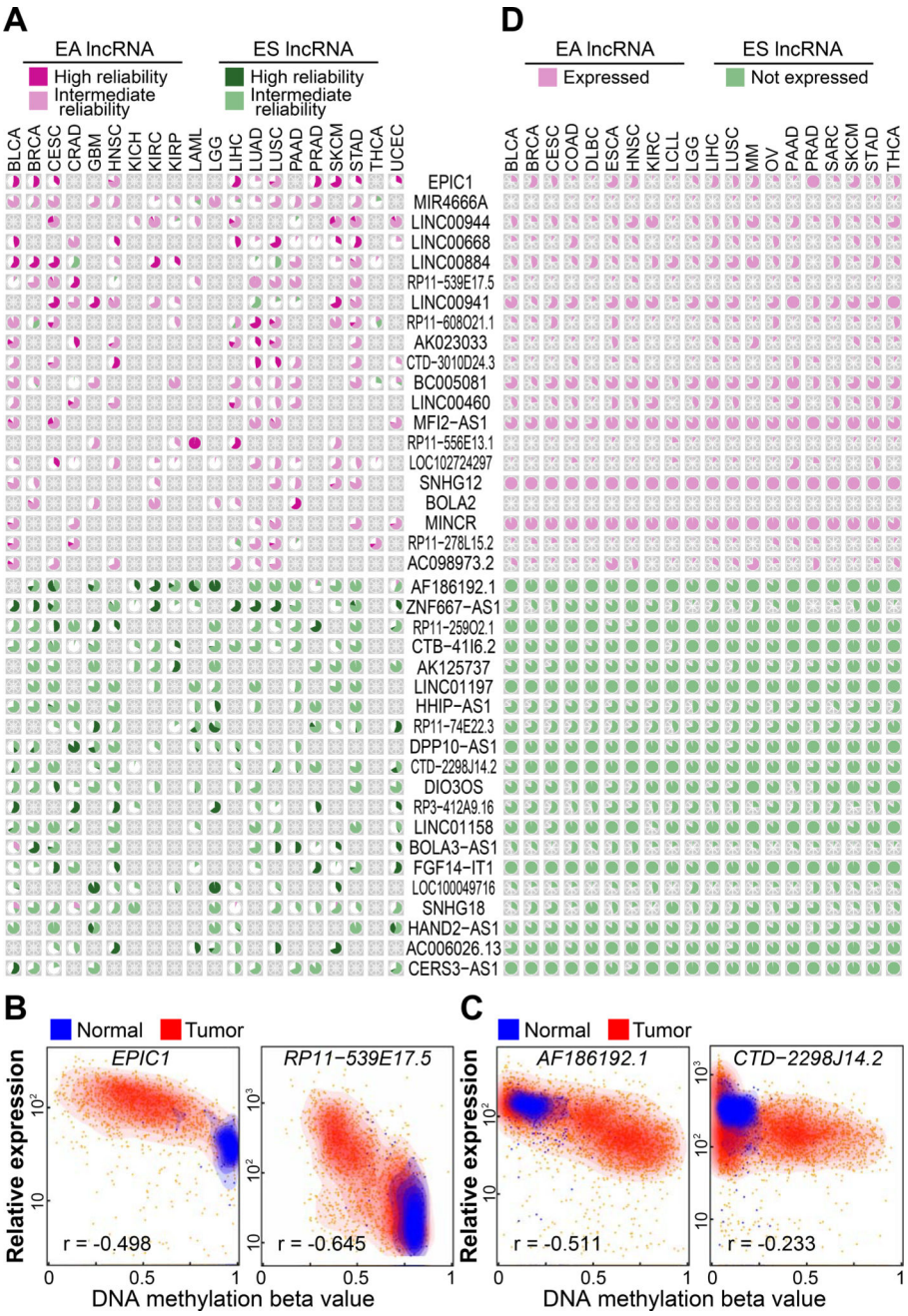

Figure 2. Epigenetic landscape of lncRNAs in cancer

(A) Percentages of significant EA (top panel) or ES (bottom panel) lncRNAs in 20 cancer types. Each pie chart indicates the percentage of each lncRNA epigenetic alteration in each cancer type. Purple indicates EA lncRNAs; green indicates ES lncRNAs. (B, C) Correlation of representative EA (B) or ES (C) lncRNAs' expression and their DNA methylation level in cancer tissues (red) and normal tissues (blue). y-axis, expression level based on RNA-seq; x-axis, DNA methylation beta value based on Infinium HM450 BeadChip.

(D) Expression of the top 20 EA (top panel) and ES (bottom panel) lncRNAs in cancer cell lines from the CCLE database. Each pie chart indicates the percentage of cell lines with the

lncRNA expressed (purple, absolute read count > 0) or not expressed (green, absolute read count = 0) in each cancer type.
See also Figure S2 and Table S2.

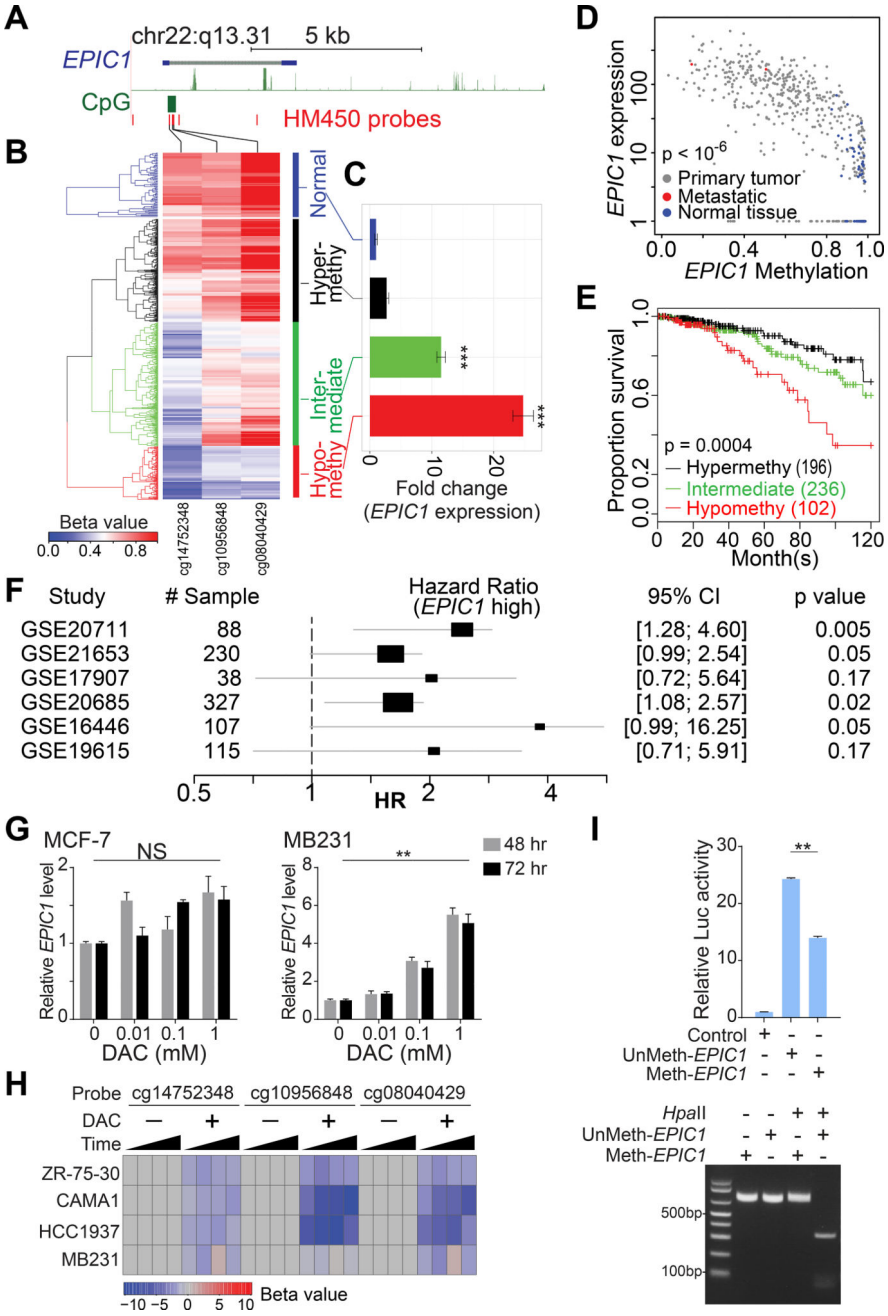

Figure 3. Expression level of *EPIC1* is regulated by DNA methylation and associated with poor survival in breast cancer patients

(A) The locations of *EPIC1* gene (blue), CpG islands (green) and HM450 probes (red) in GRCh37 reference human genome (chr22:48,027,423–48,251,349).

(B) Heatmap with beta value of DNA methylation obtained from three *EPIC1* HM450 probes in breast normal tissues and tumors. Three subgroups were identified using a hierarchical clustering analysis in tumors. Black, hypermethylation; green, intermediate; red, hypomethylation. *EPIC1*'s DNA methylation in normal tissues (blue) is shown as control. Full IDs of *EPIC1* HM450 probes are cg10956848, cg14752348 and cg08040429.

(C) Relative *EPIC1* expression in three subgroups above, compared to the level in normal tissues, respectively. ***p < 0.001.
(D) Correlation of *EPIC1* expression with *EPIC1* DNA methylation status in breast cancer and normal tissues. Probe cg08040429 represents the DNA methylation status.
(E) K–M survival curve represents the proportion survival of breast cancer patients with three subgroups above.
(F) Forest plot of *EPIC1*'s association with survival in six independent breast cancer cohorts. *EPIC1*'s expression is measured by Affymetrix 1563009_at (HG-U133_Plus_2).
(G) qRT-PCR analysis of *EPIC1* expression in MCF-7 and MB231 cells treated with decitabine (DAC).
(H) *EPIC1* methylation status detected by the same three probes (B) in breast cancer cell lines treated with decitabine. Beta value score shows the methylation status.
(I) Reporter assay of methylated and unmethylated *EPIC1* promoters (top). *In vitro* DNA methylation status of *EPIC1* promoters was confirmed by *Hpa*II restriction enzyme (bottom). Error bars indicate mean ± SD, n = 3 for technical replicates. **p < 0.01. NS, not significant. See also Figure S3.

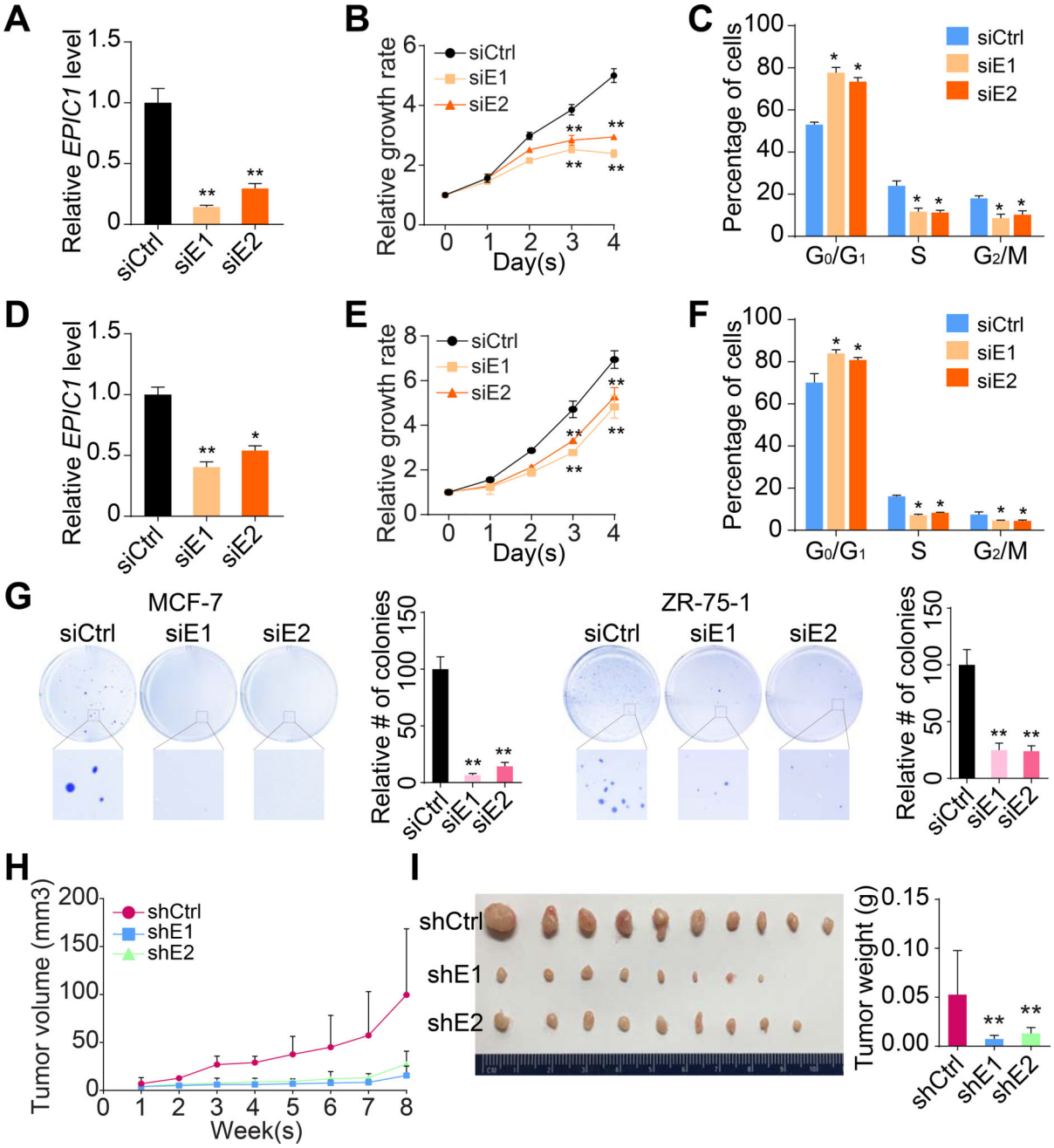

Figure 4. *EPIC1* functions as an oncogenic lncRNA in breast cancer

(A–C) qRT-PCR analysis of *EPIC1* (A), MTT assay (B), and cell cycle analysis (C) in MCF-7 cells treated with *EPIC1* siRNAs (siE1 and siE2).

(D–F) qRT-PCR analysis of *EPIC1* (D), MTT assay (E), and cell cycle analysis (F) in ZR-75-1 cells treated with *EPIC1* siRNAs.

(G) Anchorage-independent colony formation assays of MCF-7 (left) and ZR-75-1 (right) cells treated with *EPIC1* siRNAs.

(H) Quantification of tumor growth in xenograft mouse models bearing with stable *EPIC1* knockdown (shE1 and shE2) or control (shCtrl) MCF-7 cells.

Error bars indicate means ± SD, n = 3 for technical replicates. *p < 0.05, **p < 0.01. (I) Representative tumor size (left), and quantification of tumor weight (right) from xenograft mouse models. Data are presented as means ± SD (n = 10). **p < 0.01. See also Figure S4.

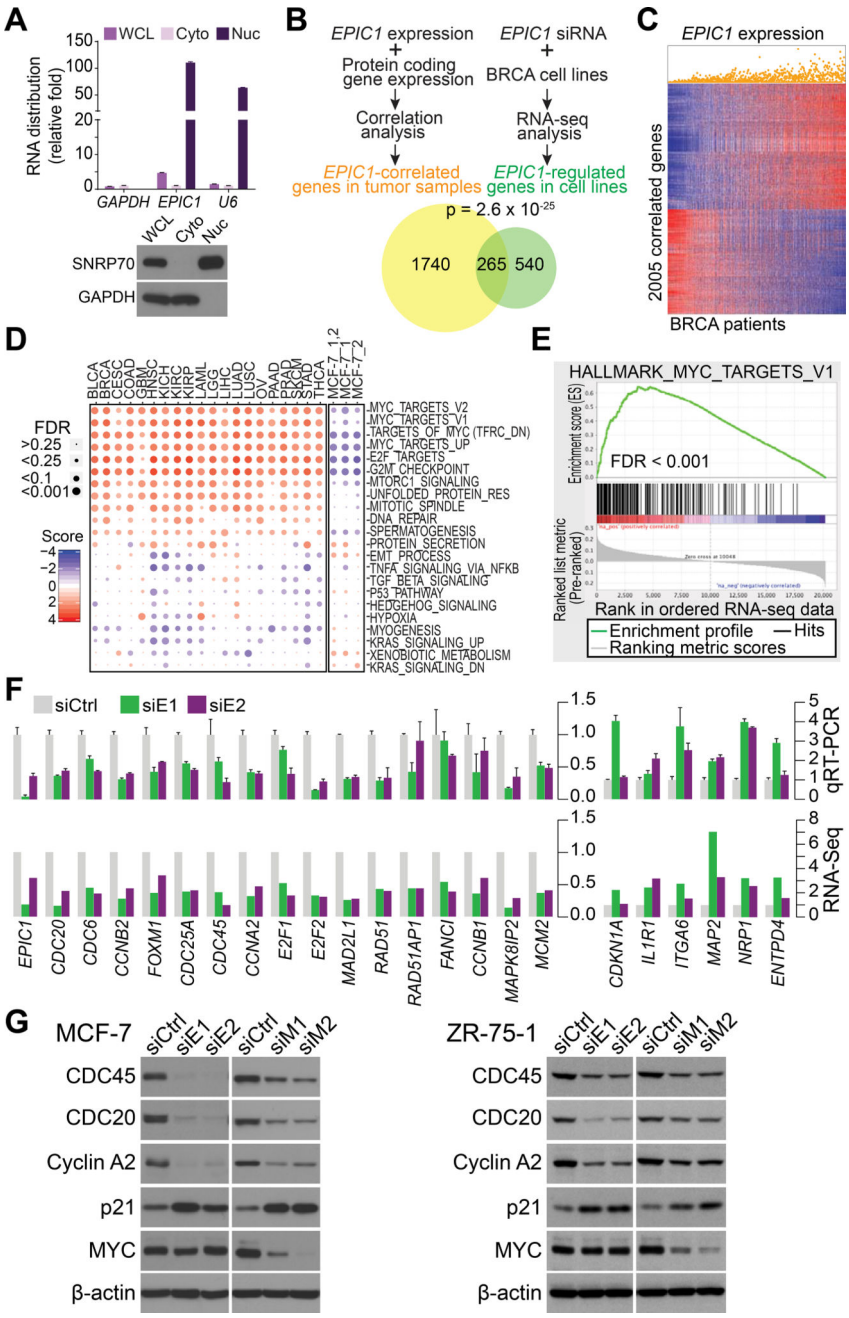

Figure 5. *EPIC1* is a nuclear lncRNA regulating MYC targets expression

(A) qRT-PCR analysis of *EPIC1* expression (top) and Western blot (bottom) of subcellular fractionation in MCF-7cells. *GAPDH* and *U6* RNA served as a marker for cytoplasmic and nuclear gene localization, respectively. SNRP70 and GAPDH served as a specific nuclear and cytoplasmic marker to whole cell lysates (WCL), cytoplasmic (Cyto), and nuclear fractionation (Nuc). Error bars indicate mean ± SD, n = 3 for technical replicates.

(B) Schematic of the identification of *EPIC1* correlated genes in breast tumors from TCGA (yellow), and genes potentially regulated by *EPIC1* in MCF-7 cells (green).

(C) Co-expression analysis showing that *EPIC1* expression is associated with 2005 genes in 559 patients with breast cancer (BRCA). Each column represents one patient.
(D) GSEA analysis of the *EPIC1*-related pathways in 20 cancer types (left panel) and *EPIC1* knockdown MCF-7 cells (right panel). The heatmap indicates the GSEA scores.
(E) Association between the enrichment of MYC targets and *EPIC1* expression in breast tumors by GSEA analysis (D).
(F) *EPIC1*-regulated gene expression by qRT-PCR analysis (top) and RNA-seq (bottom). Error bars indicate mean ± SD, n = 3 for technical replicates.
(G) Western blot of MYC-regulated targets in MCF-7 (left) and ZR-75-1 (right) cells treated with *EPIC1* and MYC siRNAs.
See also Figure S5 and Table S3.

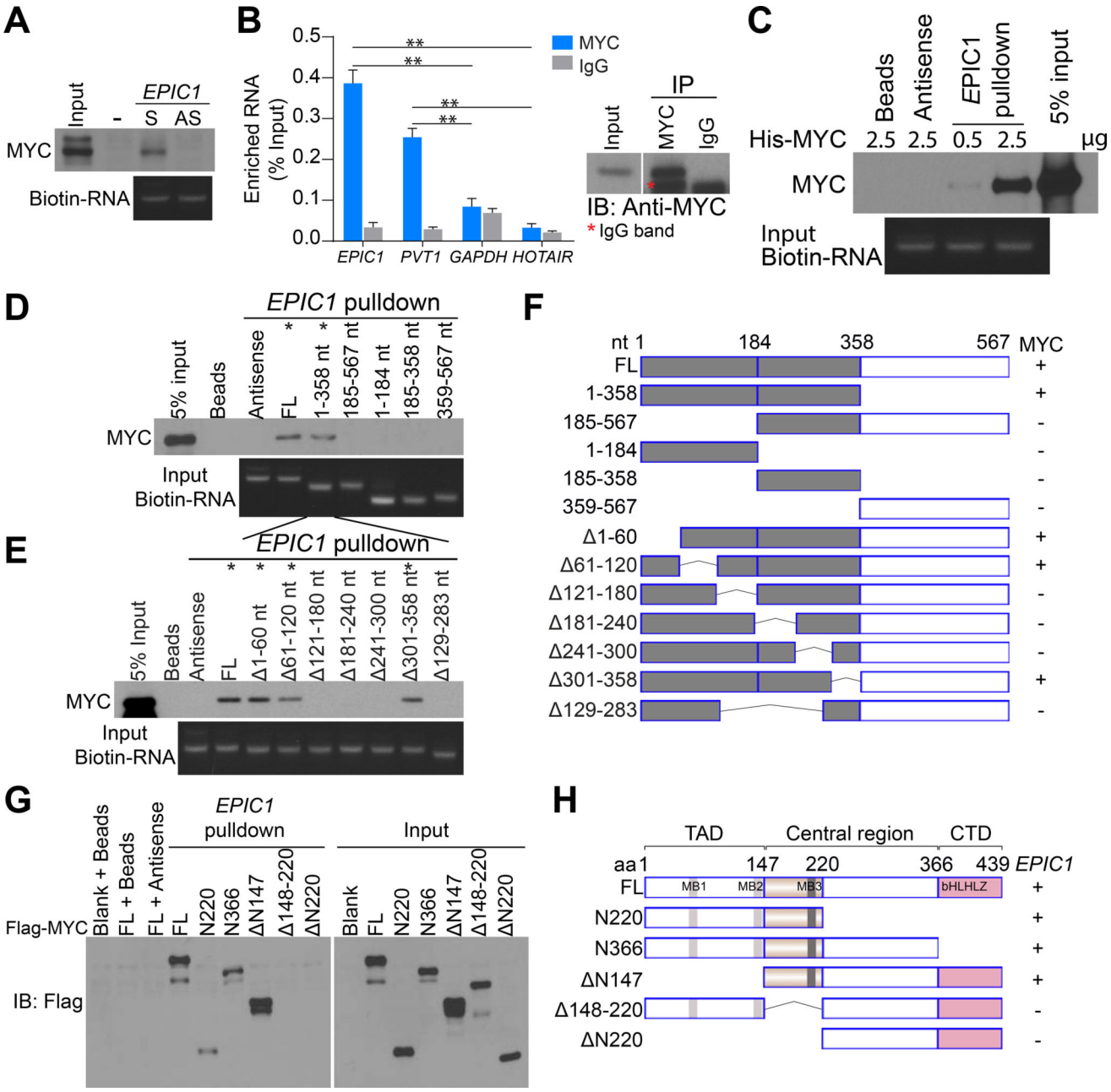

Figure 6. *EPIC1* binds directly with MYC

(A) Western blot of MYC proteins retrieved by *in vitro*-transcribed biotinylated *EPIC1* from MCF-7 cell nuclear extracts. Antisense *EPIC1* was used as a negative control. S, sense strand; AS, antisense strand.

(B) qRT-PCR analysis of *EPIC1* and *PVT1* enriched by MYC proteins in MCF-7 cells. Western blot of MYC is shown (right). *HOTAIR* and *GAPDH* served as negative controls. Error bars indicate mean ± SD, n = 3 for technical replicates. **p < 0.01.

(C) Western blot of recombinant MYC proteins retrieved by *EPIC1* RNA in *in vitro* binding assay. *EPIC1* antisense was used as a negative control.

(D) Western blot of MYC pulled-down by truncated *EPIC1.*

(E) Mapping of the MYC binding region within 1–358 region of *EPIC1*.
(F) Schematic of truncated or deletion mutants of *EPIC1*. The MYC binding capability is shown (Right).
(G) Western blot of truncated MYC proteins retrieved by *in vitro*-transcribed *EPIC1*.
(H) Schematic of truncated MYC protein. The *EPIC1* binding capability is shown. TAD, N-terminal transactivation domain; MB1-3, MYC boxes 1–3; bHLHLZ, basic-helix-loophelix-leucine zipper domain; CTD, C-terminal domain.
See also Figure S6.

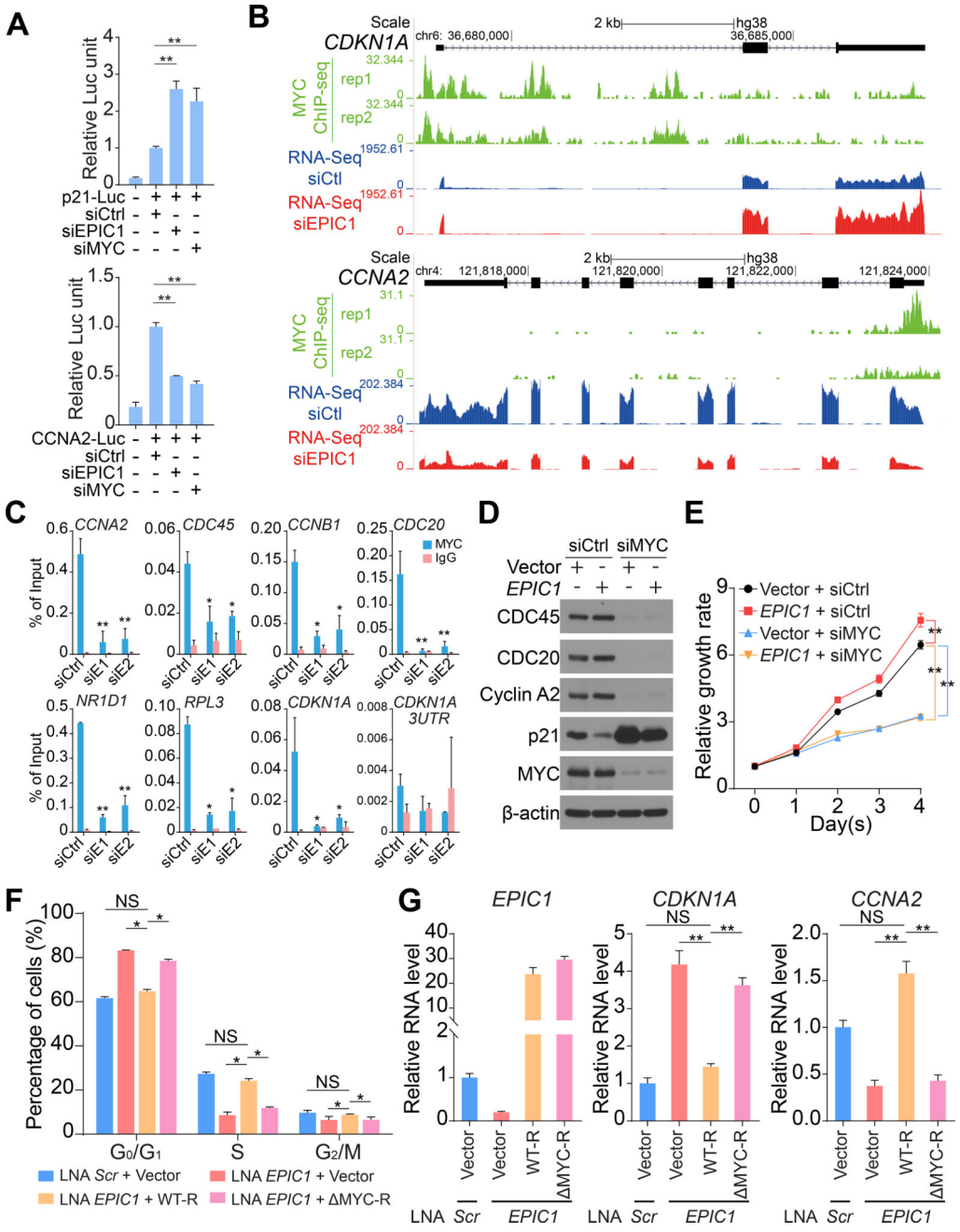

Figure 7. MYC is required for the regulatory role of *EPIC1* in cancer

(A) Reporter assay of *CDKN1A* (p21) and *CCNA2* (Cyclin A2) promoters.

(B) Alignment of two biological replicates of MYC ChIP-seq in MCF-7 cells (green) and RNA-seq from siCtrl (blue) and siEPIC1 (red) RNA treated MCF-7 cells. *CDKN1A* and *CCNA2* genomic locus are shown.

(C) ChIP-qPCR analysis of MYC occupancy on the promoters of target genes in MCF-7 cells treated with *EPIC1* siRNAs.

(D, E) Western blot of MYC targets (D) and MTT assay (E) after treatment with *MYC* siRNAs in MCF-7 cells with stable overexpression of *EPIC1* and empty vector.

(F, G) Cell cycle analysis (F) and qRT-PCR analysis of *EPIC1, CDKN1A*, and *CCNA2* level (G) in MCF-7 cells transfected with LNA against *EPIC1* followed by overexpression of indicated vectors.

Error bars indicate mean ± SD, n = 3 for technical replicates. *p < 0.05, **p < 0.01. NS, not significant.

See also Figure S7 and Table S4.